Università degli Studi di Palermo

AREA QUALITÀ, PROGRAMMAZIONE E SUPPORTO STRATEGICO
SETTORE STRATEGIA PER LA RICERCA
U. O. DOTTORATI

Dottorato di Ricerca in Medicina Molecolare e Clinica
Dipartimento di Promozione della Salute, Materno-Infantile, di Medicina Interna e Specialistica di Eccellenza "G. D'Alessandro" (PROMISE)
MED/04

Prediction of progression to symptomatic multiple myeloma in patients with high-risk plasma cell dyscrasias

IL DOTTORE
ANNA MARIA CORSALE

IL COORDINATORE
PROF. RE ANTONINO TUTTOLOMONDO

IL TUTOR
PROF.SSA SERENA MERAVIGLIA

IL CO-TUTOR
PROF.RE CIRINO BOTTA

CICLO XXXVII
ANNO CONSEGUIMENTO TITOLO 2025

Table of contents

Summary

Multiple myeloma (MM) is the second most common hematological malignancy, characterized by the clonal proliferation of plasma cells in the bone marrow (BM). It's often preceded by two preneoplastic stages, such as monoclonal gammopathy of undetermined significant (MGUS) and smoldering MM (SMM). To date, for all patients with MM, especially those classified as "high-risk", the disease remains incurable, despite advancements made in recent years in developing new therapeutic strategies. The causes of progression are currently not completely understood; however, a complex combination of clonal expansion, genetic and chromosomal aberrations, and dysregulation of the immune microenvironment are required for the development of MGUS into full-blown malignancy.

Investigating the role of the immune system in the progression of monoclonal gammopathies is critical for advancing both our understanding of MM pathogenesis and progression, and the development of more effective, early-stage therapeutic interventions. By integrating immune profiling into risk assessment and therapeutic decision-making, it may become possible to intercept the disease at its earliest stages, offering patients a significantly improved prognosis and a better chance at long-term disease control.

This project emphasizes the pivotal roles that specific myeloid and lymphoid cell subsets, along with a complex network of cytokines, chemokines, and microbiota composition, exert in driving the progression from MGUS to MM. The findings indicate that these immune cell populations are not merely passive components of the immune system; rather, they actively participate in the pathophysiological changes that characterize this transition. Additionally, these immune subsets have significant predictive value regarding patient survival, treatment response, and the duration of treatment effectiveness, especially in the context of minimal residual disease (MRD).

In summary, this project seeks to establish a foundation for identifying new biomarkers and uncovering novel therapeutic strategies that harness the immune system to improve clinical outcomes.

Introduction

Monoclonal gammopathies: evolution from preneoplastic states to full-blown multiple myeloma

Multiple myeloma (MM) is the second most common hematologic cancer with 35,780 new cases and 12,540 deaths estimated in United States in 2024 (1). This plasma cell dyscrasia is defined by the presence of myeloma-defining events (MDEs) that include the SLiM-CRAB criteria. These criteria consist of clonal plasma cells in the bone marrow (BMPCs) at 60% or greater, an involved/uninvolved serum free light chain ratio (FLC) equal to or greater than 100 (provided involved FLC level is ≥100 mg/L and urinary monoclonal protein excretion is ≥200 mg per 24 h), presence of at least two focal lesions on magnetic resonance imaging measuring at least 5 mm, hypercalcemia (serum calcium >1 mg/dl higher than the upper limit of normal or >11 mg/dl), renal failure (creatinine clearance <40 ml per minute or serum creatinine >2 mg/dl), anemia (hemoglobin value of >2 g/dl below the lower limit of normal, or a hemoglobin value <10 g/dl), and bone lesions (one or more osteolytic lesions on skeletal radiography, computed tomography (CT), or positron emission tomography-CT) (2).
The 5-year relative survival rate for MM has risen from 25% for diagnoses made in the mid-1970s to 60% for those diagnosed between 2013 and 2019, reflecting improvements across all races and ethnicities (1). Indeed, in the past two decades, innovative therapeutic drugs have significantly improved patient survival rates; however, MM remains an incurable disease.

Patients with MM typically progress from an asymptomatic pre-malignant condition known as monoclonal gammopathy of undetermined significance (MGUS). Approximately 80% of these cases arise from non-IgM MGUS, while the remaining 20% originate from light-chain MGUS (LC-MGUS), with an overall progression rate of 1% per year (2). However, more than 50% of patients with MGUS have lived with the condition for over 10 years before receiving a clinical diagnosis. To date, the diagnosis of MGUS is characterized by serum monoclonal protein (M protein) levels below 3 g/dL, the presence of less than 10% BMPCs, and the absence of SLiM-CRAB criteria. The current standard of care for these patients follows a "watch and wait" strategy, which involves regular monitoring and follow-up assessments (3). Available risk stratification models, developed by combining different prognostic factors, help identify the likelihood of progression in patients with MGUS. The Mayo Clinic (4) identified three key risk factors in MGUS: serum monoclonal (M) protein level >15 g/L, a non-IgG isotype (IgA or IgM), and an abnormal serum FLC ratio (<0.26 or >1.6). Based on the number of risk factors present, four risk categories were defined: low risk (0 factors), low–intermediate (1 factor), high–intermediate (2 factors), and high risk (3 factors), with absolute risks

of progression at 5%, 21%, 37%, and 58%, respectively. Building on this model, the Sweden study introduced immunoparesis (reduction of ≥1 uninvolved heavy chain) as an additional risk factor (5).

Further insights from the PETHEMA studies (2007 and 2020) identified additional key risk factors for progression, including an aberrant phenotype in over 95% of BMPCs, along with DNA aneuploidy or a 10% increase in M protein levels by the third year, confirmed by two consecutive measurements taken at least one month apart. The presence of two risk factors is associated with a 72% risk of progression (6,7).

In recent years, the focus on early detection and intervention in patients at risk of developing MM has led to significant advances in screening efforts. A notable example is the iStopMM study, which was launched in September 2016 and is set to conclude in 2026. This large-scale, population-based screening project involves 80,759 individuals born in 1975 or earlier in Iceland, with a total of 75,422 blood samples collected. Its primary objective is to assess the potential benefits of population-based screening for MGUS and to identify suitable candidates for justifying early intervention in MM (8). Additionally, an observational prospective study (NCT02726750) seeks to identify clinical and genomic markers that may predict why some asymptomatic patients with MGUS or SMM develop MM, while others remain unaffected.

Before progression, MGUS typically advances to a second intermediate asymptomatic condition known as smoldering multiple myeloma (SMM). This condition is characterized by serum monoclonal protein (IgG or IgA) ≥3 gm/dl, or urinary monoclonal protein ≥500 mg per 24 h and/or BMPCs 10%–60%, in the absence of SLiM-CRAB criteria or amyloidosis. Unlike patients with MGUS, individuals with SMM face a significantly higher risk of progression to symptomatic disease, estimated at approximately 10% per year during the first five years following diagnosis, 3% per year during the next five years, and 1.5% per year thereafter.

Currently, multiple risk-stratification models are available for SMM, classifying patients into low-, intermediate-, and high-risk categories. These risk-stratification models primarily focus on clinical parameters (6,10–19). The PETHEMA criteria assess risk based on two primary factors: the presence of immunoparesis (a reduction in uninvolved immunoglobulins) and the presence of more than 95% BMPCs by flow cytometry (6). In 2018, the Mayo Clinic introduced the “2/20/20” risk model, an updated framework that incorporates three key factors: serum M-protein levels above 2 g/dL, an FLC ratio greater than 20, and BMPC infiltration exceeding 20%. The 2/20/20 model has refined risk predictions, estimating a two-year progression risk of approximately 10% for low-risk, 26% for intermediate-risk, and 47% for high-risk patients (12). Subsequently, the International Myeloma Working Group (IMWG) validated the model in a large international cohort,

confirming similar two-year progression risk rates, which aligned closely with the initial estimates (10). Additionally, the model was expanded to include high-risk genetic abnormalities identified by FISH, such as t(4;14), t(14;16), del(13q), and amp(1q), as an added predictor of disease progression. This enhancement led to a refined risk model with four distinct groups, showing estimated progression risks of 4%, 26%, 51%, and 73% over two years for the low-, low-intermediate-, intermediate-, and high-risk categories, respectively, from the time of SMM diagnosis (10).

Conversely, SMM patients deemed ultra-high risk for progression (with an ≥80% risk of progression within 2 years) have been reclassified as MM (2).

The current approach to managing SMM, including high-risk cases, involves careful observation until definitive signs of progression appear. However, clinical trials are currently underway to evaluate the efficacy and safety of prophylactic therapies for high-risk SMM patients to delay or prevent the progression to symptomatic disease. These therapies include immunomodulatory drugs (IMiDs), proteasome inhibitors (PIs), and monoclonal antibodies, such as lenalidomide, bortezomib, carfilzomib, daratumumab, isatuximab, elotuzumab and dexamethasone (NCT03236428, NCT04850846, NCT02415413, NCT03301220, NCT03937635, NCT04775550, NCT03289299, NCT02960555, NCT04270409, NT01441973, NCT02279394, NCT02603887, NCT01484275) (20–32). Moreover, the phase 2 D-PRISM study investigated the effectiveness of the anti-CD38 monoclonal antibody in patients with high-risk MGUS or low-risk SMM (NCT03236428) (33).

More than genetics: the impact of the immune microenvironment on MM pathogenesis and progression

The pathogenesis of MM is a complex and multifaceted process marked by significant heterogeneity among patients. The progression of the disease is a multistep process that involves various molecular and genetic alterations (34). Key contributors to the initiation and progression of MM include chromosomal translocations, aneuploidy, and genetic mutations (e.g. mutation of genes encoding for epigenetic regulators) (35,36), as summarized in **Figure 1**.

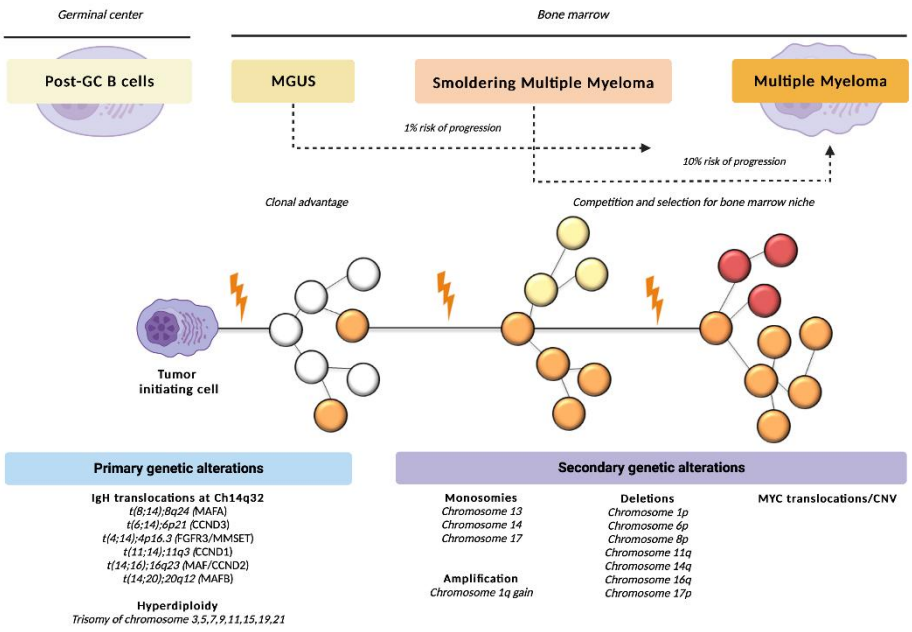

Figure 1. Genetic alterations involved in the pathogenesis of monoclonal gammopathies
Plano F., Corsale AM. et al. Hematol Rep. (2023) (37) (**See Appendix I**)

On the recent years, the tumor microenvironment (TME) is considered an evolving and intricate ecosystem that plays a key role in supporting cancer progression. It facilitates continuous, reciprocal communication between malignant BMPCs and the surrounding BM microenvironment, creating a protective niche that nurtures tumor survival. This two-way interaction not only promotes tumor growth but also contributes to increased resistance to treatments, making it harder for therapies to be effective, while simultaneously impairing the immune system's ability to detect and eliminate cancer cells (37,38).

In the context of MM, the TME becomes even more complex due to the involvement of a wide range of cellular and non-cellular components. Hematopoietic stem cells, myeloid cells, T and B lymphocytes, natural killer (NK) cells, erythrocytes, osteoclasts, and non-hematopoietic osteoblasts all actively participate in this intricate crosstalk. These cells interact with stromal components, such as fibroblasts and endothelial cells, which provide structural and functional support to the tumor.

Additionally, the TME contains acellular elements, including the extracellular matrix (ECM), which offers a scaffold for cell attachment and movement, and a variety of soluble factors like cytokines, chemokines, and growth factors. These molecules, produced by the cells within the TME, further enhance tumor growth by modulating immune responses, encouraging inflammation, and creating a favorable environment for cancer cells to thrive (37). This highly coordinated network of cellular and molecular interactions within the TME not only drives tumor progression but also creates barriers to immune surveillance. The immune system, which is normally tasked with identifying and destroying abnormal cells, becomes less effective in the presence of a TME that suppresses its function. Over time, these mechanisms contribute to immune evasion, allowing the tumor to persist and expand unchecked (**Figure 2**) (**see Appendix I**).

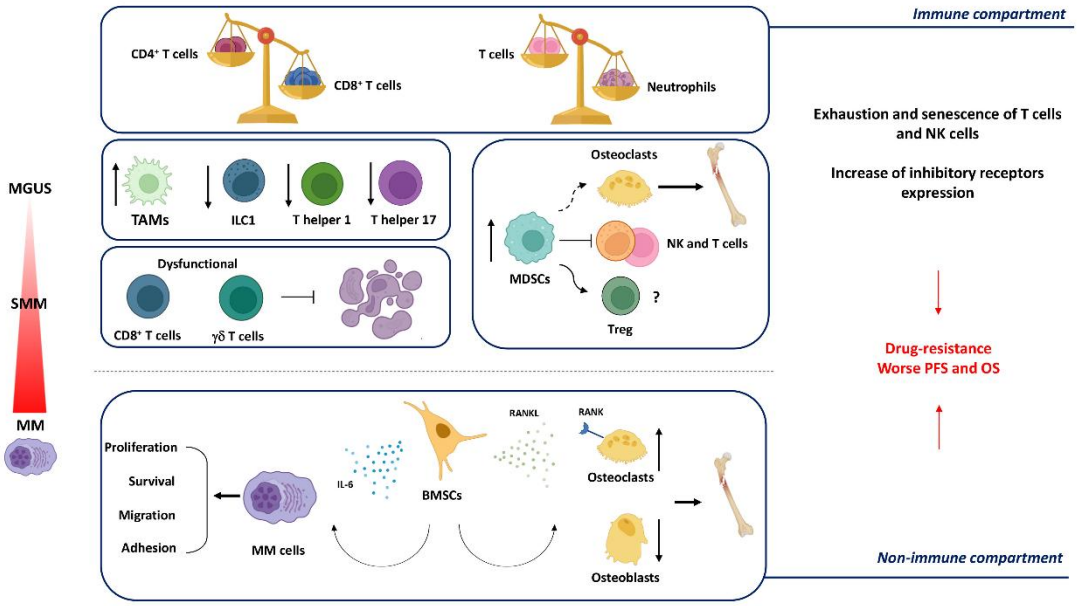

Figure 2. The immune and non-immune compartment of the BM niche in the progression from preneoplastic stages to active MM
Plano F., Corsale AM. et al. Hematol Rep. (2023) (37) (**See Appendix I**)

In patients with monoclonal gammopathies, there is a well-documented dysregulation of the immune system. This includes broad alterations in the composition and function of immune cell populations as well as changes in the cytokine milieu.

Lymphoid cells

T lymphocytes play a fundamental role in the immune system's ability to detect and control tumor growth, and their involvement in MM immunosurveillance is significant. Abnormalities in both the

quantity and functionality of T lymphocyte subsets begin to emerge early in the disease, even at the stage of MGUS (39–43). T cells in MGUS are enriched for stem-like memory T cells, overlapping in part with a quiescent tissue-resident phenotype, while T cells in MM show greater expression of lytic genes and senescence markers (44,45).

One of the hallmark features observed in MM patients is an inversion of the CD4 T cells-to-CD8 T cells ratio in both bone marrow mononuclear cells (BMMCs) and peripheral blood mononuclear cells (PBMCs), compared to healthy individuals or patients with MGUS/SMM (44,46,47). This altered ratio has been linked to poorer clinical outcomes, including shorter progression-free survival (PFS) and overall survival (OS), as well as a higher likelihood of disease relapse. Additionally, both increase or decrease in the Th1/Th2 ratio have been observed, therefore making it difficult to elucidate the clinical implications of these findings (48,49). Concerning CD4 T cells, was observed a reduction in those exhibiting a central memory phenotype, which was accompanied by an increase in naïve phenotype as MM progressed (50,51). While CD4 and CD8 T cells from patients with MGUS are capable of mounting a robust immune response against premalignant plasma cells, this ability is largely diminished in MM patients (52). This loss of functionality may be attributed to immune exhaustion. Indeed, T cells display signs of exhaustion and senescence in MM, indicated by significantly increased expression of inhibitory receptors such as PD-1, TIGIT, and CTLA-4 compared to those in MGUS/SMM or healthy individuals (HD) (42,50,53–56). Specifically, patients with a more pronounced T cell exhaustion signature or increased levels of immunosuppressive cells in their BM had worse outcomes, including shorter PFS and OS. Conversely, patients with more active cytotoxic T cells and functional antigen-presenting cells showed better responses to treatment and improved survival rates (57).

Another element that contributes to the dysfunction of CD8 T cells in MM is the modification of the antigen-processing machinery in neoplastic plasma cells. These alterations can hinder the presentation of tumor antigens, thereby making it challenging for CD8 cytotoxic T cells to identify and target malignant cells effectively. Patients with MM experience a reduction in memory CD8 T cells, which are essential for maintaining long-term immune surveillance and providing a swift response to tumor recurrence. This depletion likely impairs the immune system's capacity to sustain an effective attack on malignant plasma cells, enabling the disease to advance without adequate immune resistance. Contextually, MM patients are characterized by an increase of CD8 T cells with an effector phenotype and expressing GZMK, CCL3, CCL2, and XCL2 (50,51,58).

Furthermore, the balance between regulatory T cells (Tregs) and Th17 cells shifts, creating a more immunosuppressive environment. A higher Treg-to-Th17 ratio is linked to poorer OS because Tregs inhibit effector T cell activity, while Th17 cells, despite their role in immune responses, are

associated with pro-inflammatory and tumor-promoting effects in MM (59,60). The presence of Th17 cells has been connected to advanced disease stages and the development of lytic bone disease, a key feature of MM (61–64).

Instead, the role of Tregs in MM remains a subject of debate (65,66). Several studies have reported an increased frequency of Tregs in MM patients, which has been linked to adverse clinical features, including hypercalcemia, reduced normal plasma cell counts, elevated IgA subtype, lactate dehydrogenase (LDH), and β2 microglobulin levels. This increase is also associated with poorer treatment response, heightened infection susceptibility, and shorter PFS and OS (67–71). Moreover, Tregs were found to be elevated in patients with high-risk SMM, and two subsets of $CD39^{-}$ Tregs showed contrasting patterns in MGUS and MM, underscoring their potential role in disease progression (21,60,72). On the other hand, other studies have reported either a reduction or no significant change in Treg levels. These discrepancies might stem from differences in the types of samples analyzed, the various methods used for identifying and measuring Tregs (48,50,67–70,73–80). Despite these inconsistent findings, there is broad consensus that Tregs play a pivotal role in MM by promoting immune evasion and are notably prevalent in BM tumor sites (81).

Innate lymphoid cells (ILCs) represent one of the earliest immune cell subsets to become enriched in the TME during the progression of MM (45,82). In patients with MGUS there is a notable increase in BM group 1 ILCs that produce IFN-γ, and a reduction in IL-13–producing group 2 ILCs. However, as the disease progresses to SMM, the frequency of these IFN-γ–producing group 1 ILCs begins to decline.

As MM progresses, particularly in advanced stages, a marked decrease in NK cell frequency is observed in patients with poor prognosis, as compared to healthy controls and MGUS patients. Their reduced presence in MM suggests a compromised immune response that could contribute to disease progression. The functional impairment of NK cells in MM is further compounded by the TME, which suppresses their ability to effectively eliminate BMPCs. This suppression is mediated by a downregulation of key activating receptors on NK cells, such as CD16, NCR3/NKp30, NKG2D, CD244/2B4/p38, and DNAM-1, which are critical for recognizing and destroying cancer cells. Simultaneously, the TME promotes an upregulation of inhibitory receptors on NK cells, including KIR2DL1, PD1, TIM3, and TIGIT. This shift in the balance between activating and inhibitory signals significantly impairs NK cell-mediated cytotoxicity, rendering them less effective at controlling MM progression (83–85).

Myeloid cells

Numerous studies have highlighted the critical role of tumor-associated macrophages (TAMs) as key contributors to the onset and progression of MM, particularly those resembling M2-polarized macrophages (86–88). These TAMs represent about 10% of the BM in patients with MM, highlighting their significance within the TME (89). TAMs are associated with MM pathophysiology, disease progression, immunosuppression and drug resistance (86,87). Increased levels of CD163+ or CD206+ TAMs serve as negative prognostic indicators in MM, with heightened frequencies linked to more aggressive forms of the disease (90–94). Additionally, patients who fail to achieve complete remission tend to have higher TAM counts, and there is a positive correlation between treatment response and the number of TAMs at diagnosis (81).

In addition to TAMs, myeloid-derived suppressor cells (MDSCs) are also involved in the pathogenesis and progression of MM (95–98). These cells engage in complex bidirectional interactions with myeloma cells, contributing significantly to both tumor progression and immune suppression. They can secrete soluble factors such as cytokines and chemokines that not only influence the behavior of myeloma cells but also modulate the activity of other immune cells present in the TME. For example, the production of interleukin-6 by myeloma cells can promote the survival and expansion of MDSCs, while MDSCs can, in turn, release factors that enhance myeloma cell proliferation and survival (99). Furthermore, the interactions between MDSCs and myeloma cells are not unidirectional; they often involve feedback loops that reinforce the immunosuppressive and tumor-promoting features of both cell types. For instance, MDSCs can express programmed cell death ligand 1 (PD-L1), which inhibits T cell activity, thereby allowing myeloma cells to evade immune detection and destruction. This creates an environment where myeloma cells can thrive, leading to increased disease aggressiveness and resistance to treatment (100). Additionally, MDSCs are known to promote angiogenesis, which is critical for tumor growth and metastasis. By secreting pro-angiogenic factors, MDSCs can stimulate the formation of new blood vessels, thereby enhancing the nutrient supply to myeloma cells and facilitating tumor expansion (98).

Their accumulation in the BM is detectable even in patients with MGUS and persists throughout the course of the disease, including during periods of remission. Within this context, polymorphonuclear MDSCs (PMN-MDSCs) are the predominant subpopulation in both MGUS and MM, while other research indicates that monocytic MDSCs (M-MDSCs) are more prevalent at diagnosis and during relapse. Immunogenomic analyses have identified $CD11b^{+}$ $CD13^{+}$ $CD16^{+}$ cells as the PMN-MDSC subset with the most significant ability to suppress T-cell responses (101).

Neutrophils are also significantly elevated in the BM and peripheral blood of patients with MM. These cells contribute to immunosuppression, support tumor growth, and promote resistance to

treatment, thereby exacerbating the progression of MM. Their increased presence within the TME not only facilitates myeloma cell survival but also undermines the effectiveness of therapeutic strategies. Impairments in neutrophil maturation, including diminished lysozyme activity and elevated levels of arginase (e.g. arginase 1), have been reported in MM as a result of increased susceptibility to infections and contributed to the immunological dysfunction that promotes tumor progression (102). High-density neutrophils from MM and MGUS exhibited upregulation of CD64 and downregulation of CD16, alongside diminished phagocytic activity and reduced oxidative burst (102). The neutrophil-to-lymphocyte ratio (NLR) is elevated in certain patients with MM and has been employed as a prognostic indicator for various groups, including those who have previously undergone autologous hematopoietic stem cell transplantation (aHSCT), and transplant-ineligible individuals. This ratio serves as a valuable tool for predicting clinical outcomes and guiding treatment decisions in the management of MM (103–106).

During the transition from MGUS to MM, dendritic cells (DCs) experience notable changes in phenotype and function. DCs displayed impaired antigen-presentation capabilities, with reduced expression of co-stimulatory molecules and critical markers such as HLA-DR (57). In MM patients, there is a 50% reduction in myeloid DCs ($BDCA1^+$) and plasmacytoid DCs (pDCs) ($BDCA2^+$) within PBMCs compared to healthy individuals, and this reduction occurs independently of the disease stage (107–109). Conversely, in the BM there is an accumulation of myeloid DCs ($CD11c^+$) and pDCs ($CD11c^-$ $CD123^+$) in MM patients compared to those with MGUS, indicating an increased tumor burden (110–112).

Additionally, peripheral myeloid DCs and pDCs in MM patients display reduced expression of critical markers, including CCR5, CCR7, DEC-205, HLA-DR, and co-stimulatory molecules, as well as lower levels of IFN-γ production (107,108). This contributes to defective T cell proliferation and activation, likely due to impaired migration and antigen capture by these DCs.

During the MGUS-to-MM transition, a key finding is the progressive increase in CD28 expression on tumor plasma cells. CD28, a receptor for CD80/CD86, mediates interactions with BM myeloid DCs, leading to a reduction in proteasome subunit expression in the tumor cells, which helps them evade $CD8^+$ T cell-mediated destruction (110). However, some studies have reported normal DC counts in MM patients, suggesting variability in DC-related findings across different studies (113).

Aims and research objectives of the thesis

This project focuses on advancing personalized and non-invasive approaches for monitoring and identifying therapeutic targets in MM. By utilizing innovative technologies, it aims to enable the early detection of patients with asymptomatic monoclonal gammopathies, specifically MGUS and SMM, with a focus on those at high risk of progressing to symptomatic MM. These conditions, if left undetected, can progress to MM, which significantly impacts patient health and clinical outcomes.

Genetic alterations identified in MM patients are frequently detectable in pathological plasma cells during the early stages of asymptomatic monoclonal gammopathies. This observation suggests that, beyond the inherent genetic changes within the neoplastic cells, other "extrinsic" factors are likely involved in regulating the delicate balance between the latency and progression of pre-neoplastic stages. Among these extrinsic factors, the immune system is known to influence either containing or promoting disease progression significantly.

Thus, the research objectives of this project focus on exploring the role of specific myeloid and lymphoid cell subsets in the immunopathogenesis of MM and its preneoplastic stages, evaluating their functional properties and understanding how the TME shapes their activity and behavior. A deeper understanding of these interactions is essential for identifying patients with pre-malignant or asymptomatic plasma cell dyscrasias who are at high risk of progression to MM. By uncovering the mechanisms that drive the transition from a latent to an active disease state, this knowledge could lead to the development of more precise, personalized strategies for early intervention. Such strategies could involve monitoring high-risk patients more closely, employing novel immunomodulatory therapies, or targeting the TME to prevent disease progression. Ultimately, this would allow for more effective management of high-risk patients, significantly improving their prognosis and clinical outcomes by preventing or delaying the onset of symptomatic MM.

Materials and Methods

Patients 'enrollment

Patient recruitment and sample collection were conducted in accordance with the Declaration of Helsinki. Ethical approval for the collection of human samples for research purposes was obtained from the Institutional Review Board of A.O.U.P. Azienda Ospedaliera Policlinico Paolo Giaccone in Palermo (approval number 02/2022, project code: MMVision). All participants provided informed consent, confirming that the donation of specimens for this research would not impact their diagnosis, treatment, or prognosis. This work was supported by a grant from the Italian Association for Cancer Research (AIRC) within the My First AIRC Grant 2020 (n. 24534, 2021/2025).

Isolation of peripheral blood and BM mononuclear cells

All blood samples and BM aspirates, obtained at diagnosis and before the initiation of treatment, were collected in ethylenediaminetetra-acetic acid (EDTA) tubes, and peripheral blood mononuclear cells (PBMCs) and BM mononuclear cells (BMMCs) were isolated using Ficoll-Paque PLUS density gradient centrifugation from MGUS, SMM and MM patients. PBMCs were also isolated from buffy coats or blood samples obtained from healthy donors (HD).

In summary, the blood samples were diluted with an equal volume of Dulbecco's phosphate-buffered saline (DPBS), and the diluted blood was carefully layered over the Ficoll to minimize mixing. Centrifugation at 400-500 g for 30 minutes at room temperature, without brakes, facilitates the separation of PBMCs or BMMCs from other blood components. The mononuclear cells form a distinct white interface, the buffy coat, between the plasma and the Ficoll. After collection, the mononuclear cells were washed with DPBS and centrifuged twice at 400 g for 5 minutes each. The cells were then resuspended in an appropriate volume of culture medium and counted.

Isolation of peripheral neutrophils and BM-derived granulocytes

Peripheral neutrophils and BM-derived granulocytes were isolated and purified following the procedure described by Cui et al. (114). Briefly, after performing density gradient centrifugation, neutrophils were in the lower layer, close to the red blood cell (RBC) fraction due to their higher density. To selectively lyse and remove RBCs while preserving granulocytes, repeated RBC lysis steps were carried out using 1X RBC lysis buffer (prepared by diluting 10X RBC lysis buffer: 1.55 M NH_4Cl, 120 mM $NaHCO_3$, 1 mM EDTA in ddH2O). If the cell pellets appeared white or contained a thin red ring on top of the pellet, the supernatant was carefully aspirated, and the cell pellet was washed with DPBS. The cells were centrifuged at 500 g for 5 minutes at 18°C–22°C. After

centrifugation, the supernatant was gently removed, and the cell pellet was resuspended in DPBS or culture media for further use.

Isolation of γδ T cells from buffy coats

γδ As previously described, t cells were enriched from PBMCs, obtained from buffy coats of healthy blood donors, through magnetic cell isolation utilizing the TCR γ/δ+ T Cell Isolation Kit Human according to the manufacturer's instructions. The non-γ/δ T cells are labeled indirectly using a cocktail of biotinylated monoclonal antibodies combined with anti-Biotin Microbeads. When placed in the magnetic field of a MACS Separator, the magnetically labeled non-TCR γ/δ+ cells are captured within a MACS® Column, while the unlabeled γ/δ T cells continue to flow through the column. The purity, approximately 90%, and the initial phenotype were assessed using flow cytometry.

Cell lines

The human MM cell lines RPMI 8226, H929, U266, and AMO were grown in T75 flasks in complete culture medium (StableCell™ RPMI-1640 with stable glutamine and sodium bicarbonate, supplemented with 25 mM HEPES buffer, 100 IU/mL penicillin, 0.1 mg/mL streptomycin, and 10%, 10%, 15%, and 20% heat-inactivated fetal bovine serum (FBS), respectively. The cultures were maintained within the cell concentration range of 3x10^5 to 1x10^6 viable cells/mL, with medium replenishment occurring 3 times weekly.

Co-cultures

PBMCs and purified γδ T cells obtained from HD were co-cultured with MM cell lines (RPMI 8226, H929, U266) at an Effector (E) to Target (T) ratio of 4:1 for 24h, 48h, and 72h in a 96-well plate. In a second experiment, PBMCs were co-cultured with MM cell lines (RPMI 8226, H929, U266, and AMO) in a 96-well plate for 5 days, maintaining an Effector (E) to Target (T) ratio of 4:1. This was conducted both in the presence and the absence of TGF-β (2 ng/mL), and accompanied by the addition of conditioned medium derived from MM cell cultures. Following, the cells were harvested and stained.

Cytotoxic assays

Peripheral neutrophils and PBMCs obtained from HD were co-cultured with MM cell line AMO at Effector (E) to Target (T) ratios of 1:1, respectively, for 24 hours in a 96-well plate, with or without Daratumumab (10 µg/mL). Following co-culture, cells were harvested, washed in cold Stain Buffer,

and stained with the following fluorochrome-conjugated antibodies: Annexin-V, 7-AAD, anti-human CD15, anti-human CD138, and anti-human CD45.

Subsequently, BMMCs and granulocytes were isolated from BM samples of untreated newly diagnosed MM patients. To assess the ex-vivo cytotoxicity of BM-derived granulocytes in combination with Daratumumab against autologous MM cells, BM-derived granulocytes were added to BMMCs at increasing concentrations, namely 1:10 and 1:2 of the original amount, up to reconstitute the original abundance (1:1) and cultured for 4 hours in a 96-well plate, both in the presence and absence of Daratumumab (10 µg/mL), and Count Bright™ Absolute Counting Beads were added. Following co-culture, cells were harvested and stained with the following fluorochrome-conjugated antibodies: Annexin-V, 7-AAD, anti-human CD138, anti-human CD45, and anti-human CD56. The killing ratio of MM cells was calculated as indicated:

$$\frac{(Absolute\ number\ of\ MM\ cells\ /absolute\ \ number\ of\ total\ lymphocytes\ in\ Daratumumab\ treated\ conditions)}{(Absolute\ number\ of\ MM\ cells\ \ /absolute\ \ number\ of\ total\ lymphocytes\ in\ untreated\ conditions)}$$

Flow cytometric analysis

PBMCs and BBMCs were washed in cold Stain Buffer and, subsequently, stained with the following fluorochrome-conjugated antibodies' panels:

CD4 T cells									
anti-human CCR6	anti-human CD25	anti-human CD161	anti-human CXCR3	anti-human CRTH2	anti-human CD127	anti-human CD3	anti-human CCR7	anti-human CD4	anti-human CD45RA
CD8 T cells									
anti-human CD57	anti-human TIM3	anti-human TIGIT	anti-human CD27	anti-human LAG3	anti-human PD-1	anti-human CD3	anti-human CCR7	anti-human CD8	anti-human CD45RA
NK cells									
anti-human CD57	anti-human TIM3	anti-human TIGIT	anti-human CD56	anti-human CD16	anti-human PD-1	anti-human CD3	anti-human NKG2A	anti-human CD45	anti-human CD8
γδ T cells									
anti-human Vδ1	anti-human TIM3	anti-human TIGIT	anti-human CD27	anti-human LAG3	anti-human PD-1	anti-human CD3	anti-human Vδ2	anti-human CD69	anti-human CD45RA
Myeloid cells									
anti-human CD16	anti-human CD274	anti-human CD39	anti-human CD33	anti-human CD11b	anti-human CD123	anti-human CD14	anti-human HLA-DR	anti-human CD45	anti-human CD11c
Functional									
anti-human Vδ1	anti-human IL17	anti-human IFN-γ	anti-human IL-4	anti-human TNF-α	anti-human IL-10	anti-human CD3	anti-human Vδ2	anti-human CD4	anti-human CD8

Following staining, the cells were incubated for 20 min at room temperature in the dark. Then, cells were washed and resuspended in 400 µl Stain Buffer before the acquisition.

Contextually, BM samples of MGUS, SMM, MM (at baseline and after therapy follow-up) were stained according to the manufacturer's guidelines, using the BD OneFlow™ PCD and Plasma Cell Screening Tube (PCST). BD OneFlow™ PCD consists of single-use tubes containing the following fluorochrome-conjugated antibodies in an optimized dried formulation: anti-human CD38 FITC, anti-human CD28 PE, anti-human CD27 PerCP Cy5.5, anti-human CD19 PE-Cy7, anti-human CD117 APC, anti-human CD81 APC-H7, anti-human CD45 BD Horizon V450, and anti-human CD138 BD Horizon V500-C antibodies. Instead, BD OneFlow™ PCST consists of two single-use tubes: PCST (S) which contains anti-human CD38 FITC, anti-human CD56 PE, anti-human β2-microglobulin PerCP Cy5.5, anti-human CD19 PE-Cy7, anti-human CD45 BD Horizon V450, anti-human CD138 BD Horizon V500-C, and PCST (C) which contains anti-human Kappa APC, and anti-human Lambda APC-H7 antibodies. Following staining, the cells were incubated for 20 min at room temperature in the dark. Cells were washed and resuspended in 400 µl Stain Buffer before the acquisition. All analyzed samples were acquired using the BD FACSLyric™ Flow Cytometer and analyzed with FlowJo software (version 10.5.3) and Infinicyt software (version 2.0.6).

Evaluation of cytokine production

PBMCs and BMMCs were cultured at a concentration of 5×10^5 cells/mL in 24-well plates in a complete culture medium (StableCell™ RPMI-1640 with stable glutamine and sodium bicarbonate, supplemented with 25 mM HEPES buffer, 100 IU/mL penicillin, 0.1 mg/mL streptomycin, and 10% heat-inactivated fetal bovine serum. To study the intracellular expression of cytokines IFN-γ, IL-17, TNF-α, IL-10, and IL-4, PBMCs and BMMCs were stimulated for 24h with ionomycin (1 µg/mL) and phorbol 12-myristate 13-acetate (PMA) (150 ng/mL) in the presence of 10 µg/mL Monensin added 1h after stimulation. After the incubation, the cells were harvested, washed with Stain buffer and surface stained using the following fluorochrome-conjugated monoclonal antibodies: anti-human Vδ1, anti-human CD3, anti-human Vδ2. Intracellular cytokine expression was evaluated upon fixation and permeabilization using the Inside Stain Kit according to the manufacturer's instructions. Monoclonal antibodies anti-human TNF-α, anti-human IFN-γ, anti-human IL17, anti-human IL-10, and anti-human IL-4 were used to stain intracellular targets. Following staining, the cells were incubated for 20 min at room temperature in the dark. Cells were washed and resuspended in 400 µl Stain Buffer before the acquisition.

Dimensionality reduction, clustering, and visualization with FlowCT

FlowCT (version 1.0.0), a semi-automated workflow for the deconvolution of immunophenotypic data and objective reporting on large datasets (115), was applied to identify possible differences in the immune microenvironment along MM evolution. The FlowSOM and Seurat clustering approaches were used for automated clustering. The median expression of each marker on multi-uniform manifold approximation and projection (UMAP) and the Infinicyt software were used to characterize each cluster.

Microbiota analysis from fecal samples

Fecal samples were collected from patients at diagnosis, obtaining 1 sample for each subject, including 10 MGUS, 15 SMM, 16 MM. Fecal samples were collected in sterile tubes, stored in a refrigerated container and delivered to the Medical Molecular Microbiology and Antibiotic Resistance Laboratory (MMARLab), Department of Biomedical and Biotechnological Sciences BIOMETEC of the University of Catania for DNA extraction and sequencing.

DNA from fecal samples was extracted with the QIAamp PowerFecal Pro DNA Kit, according to the manufacturer's protocol, which included a step of mechanical cell lysis with a bead-beating technology. Quality and quantity of extracted DNA was checked by NanoDrop 2000 Spectrophotometer and the final concentration was confirmed by Qubit 2.0 fluorometer (dsDNA HS assay). Bacterial DNA was amplified using the V3-V4 region of the 16S rRNA gene, PCR products were purified and paired-end (2×300) sequencing was performed using Illumina MiSeq as described by Ragusa et al. (116).

QIIME2 (version qiime2-2021.11) pipeline (117) was used to process the generated raw FASTQ files. At first the paired-end sequences were imported and demultiplexed, then quality filtering was performed with the deblur denoise-16S method (118) cutting to a quality score of 30. Afterwards, a feature table was constructed, and alpha and beta diversity were obtained by calculating Shannon entropy and performing Jaccard PCoA. Taxonomy was assigned to the OTUs using the Greengenes Database (version 13.8) at 99% identity. Phylum, genera, and species tables were also built, collapsing the feature table and the taxonomy. Differential abundance analyses were performed using R packages mia (version 1.10.0) (119), miaViz (version 1.10.0) (120), miaTime (version 0.1.22), NetCoMi (version 1.1.0) (121), and MicrobiotaProcess (version 1.14.1) (122).

Luminex assays

Plasma samples were collected from blood and BM aspirates of 12 MGUS, 12 SMM, and 12 MM patients. All samples were stored at –80°C until analysis. The Bio-Plex Pro Human Cytokine Screening 48-Plex Panel (Bio-Rad) was used, following the manufacturer's instructions. This panel

includes the measurement of various cytokines and chemokines, such as FGF basic, Eotaxin, G-CSF, GM-CSF, IFN-γ, IL-1β, IL-1rα, IL-1a, IL-2Rα, IL-3, IL-12 (p40), IL-16, IL-2, IL-4, IL-5, IL-6, IL-7, IL-8, IL-9, GRO-α, HGF, IFN-α2, LIF, MCP-3, IL-10, IL-12 (p70), IL-13, IL-15, IL-17A, IP-10, MCP-1 (MCAF), MIG, β-NGF, SCF, SCGF-β, SDF-1α, MIP-1α, MIP-1β, PDGF-BB, RANTES, TNF-α, VEGF, CTACK, MIF, TRAIL, IL-18, M-CSF, TNF-β.

Briefly, plasma samples were centrifuged at 10,000 g for 10 minutes at 4°C to remove platelets and precipitates, then diluted fourfold with Sample Diluent HB. 50 µL of 1X beads were added to each well of the assay plate and washed twice with 100 µL of Bio-Plex Wash Buffer. Next, 50 µL of standards, samples, and controls were added to the respective wells. The plate was incubated at room temperature for 30 minutes on a shaker set to 850 rpm. After incubation, the plate was placed on a magnetic separator, and the beads were then washed three times with 100 µL of Wash Buffer. Subsequently, 25 µL of 1X detector antibody was added to each well, and the plate was incubated for 30 minutes with shaking at 850 rpm at room temperature in the dark. The supernatant was removed, and the beads were washed three times with 100 µL of Wash Buffer. Then, 50 µL/well of Streptavidin-Phycoerythrin conjugate was added, followed by a 10-minute incubation with shaking at 850 rpm at room temperature in the dark. After removing the supernatant, the beads were washed three more times with 100 µL of Wash Buffer. Finally, 125 µL of assay buffer was added to each well, the plate was incubated for 30 seconds with shaking at 850 rpm at room temperature in the dark, and the results were immediately analyzed using a Bio-Plex Luminex 200 analyzer (Bio-Rad) and Bio-Plex Manager Software (version 6.0).

Survival analysis

To assess the prognostic value of identified immune populations in MM patients, we calculated the progression-free survival (PFS) and survival analysis was performed with the R package survival (version 3.5-8) and the function *surv()*. Kaplan-Meier curves were plotted using the function *ggsurvplot* within the R package survminer (version 0.4.9). The log-rank test is used for statistical significance and the prognosis was determined by analyzing PFS, of which starting point was first-line treatment initiation. Patients were stratified into groups according to the median value of each cell type in the whole population. The hazard ratio (HR) was also calculated to quantify the relative risk of disease progression between the stratified groups.

Gene Set Analysis

Bulk RNA-seq from CD138-positive fraction of BMMC were analyzed from a total of 859 samples coupled with clinical data, provided by the Multiple Myeloma Research Foundation (MMRF) CoMMpass study (NCT01454297). Patients were grouped according to autologous stem cell

transplantation (ASCT) eligibility: ASCT eligible = 420, median age = 60 not eligible for ASCT= 439 and, median age = 67. Firstly, a ferritin related gene-set including 49 genes was developed by merging gene ontology and Molecular Signatures Database (MSigDB). Lastly, enriched Gene Ontology (GO) terms from the biological processes and Kyoto Encyclopedia of Genes and Genomes (KEGG) pathways for the selected genes (ferritin biosynthesis) was obtained using ClueGO plug-in of Cytoscape (version 3.9.1) (123).

These gene set libraries were used as the backbone for all subsequent analysis. RNA-seq data of all MM subjects were pre-processed, log2-transformed, and analyzed using the DEseq2 R package. BiomaRt (version 2.48.2) was used for annotation based on GRCh37/hg19 to cross-map gene symbol identification. The final count matrix contained 19282 fragments per kilobase million (FPKM) and was projected in the Seurat object, where after feature selection and scaling of the normalized data, we performed principal component analysis (PCA) linear dimensional reduction. The first 20 principal components (PCs) were used to construct the k-nearest neighbor (KNN) graphic, and the Louvain algorithm was performed for clustering the patients with a resolution parameter set to 0.5. The UMAP method was applied for the non-linear dimensional reduction to visualize the entire dataset.

Cell cycle phases were scored using the list of cell cycle markers from Tirosh et al. that are preloaded in Seurat (124). Gene set enrichment analysis (GSEA) was performed using the FGSEA R package (version 1.25.1) to determine whether single cell RNA sequencing (scRNA-seq) data from bulk GEP that can be used to classify individual patients based on the developed Ferritin gene-set. The final patients clustering was used to gene set enrichment to the Kaplan–Meier survival analysis and to discover the relationships between clinical features and ferritin related genes alteration.

Single-cell RNA sequencing and pseudo-bulk analyses

Data from MGUS, SMM and MM patients were retrieved from GSE145977 (125), GSE124310 (43) and GSE163278 (45) datasets. scRNAseq results were extracted and merged using the R package Seurat (version 5.1.0). Batch removal has been performed through the Harmony package. Ferritin light chain (FTL) and ferritin heavy chain 1 (FTH1) genes were retrieved from each patient, and the mean value among all cells was used as the patient value. Patients were dichotomized according to FTH1 and FTL1 median values, and a double analysis was performed to identify associations between high and low levels of either FTL or FTH1 mRNA and immune cell composition.

The scRNA-seq, followed by the generation of pseudo-bulk RNA-seq data, was performed on BM samples, obtained from patients with MGUS (n=3), SMM (n=5), and MM (n=10), along with HDs (n=4). Samples were processed using the 10X Genomics following the manufacturer's instructions

(Chromium Next GEM Single Cell V(D)J v1.1 protocol rev F for human samples). Quality control was performed with Qubit Fluorometric Quantification using the double-stranded DNA high-sensitivity assay kit, and with TapeStation using high-sensitivity screentapes. Libraries were sequenced on a NextSeq 550 system with the sequencing depth and run parameters indicated by 10X Genomics instructions.

In scRNA-seq analysis, the immune cell annotations have been performed according to Seurat guidelines by evaluating cell projection to a reference dataset.

Statistical analysis

Statistical analysis and data visualization were conducted using R software (version 4.4.2). To evaluate intergroup differences, a range of statistical tests was employed based on data distribution and experimental design. For normally distributed data, the T-test was applied for comparing two groups, while ANOVA (Analysis of Variance) was used for comparing multiple groups. For non-normally distributed data, the Kruskal-Wallis's test was utilized for comparisons across multiple groups, and the two-sample Wilcoxon test (also known as the Mann-Whitney U test) was employed for pairwise comparisons. Statistical significance was defined as a p-value <0.05. Additionally, appropriate post-hoc tests were performed following ANOVA or Kruskal-Wallis to identify specific group differences.

All reagents, antibody and other technical information were summarized in **Table 1**.

Table 1. Reagents, instruments and software used

Antibodies and reagents for flow cytometry

Antibodies	Fluorochrome	Clone	Source	Cat. number
Mouse anti- human Annexin-V	PE	-	Miltenyi Biotec	130-118-363
Mouse anti- human Annexin-V	FITC	-	Miltenyi Biotec	130-093-060
7-AAD Staining Solution	-	-	Miltenyi Biotec	130-111-568
Mouse anti-human CD15	FITC	MMA	BD Biosciences	347423
Mouse anti-human CD138	APC	MI15	BD Biosciences	347193
Mouse anti-human CD45	V500	HI30	BD Biosciences	560777
Mouse anti-human CD138	PE	MI15	BD Biosciences	552026
Mouse anti-human CD56	PE-Cy7	NCAM16.2	BD Biosciences	335826
Mouse anti-human Vδ1	FITC	REA173	Miltenyi Biotec	130-118-362
Mouse anti-human CD3	APC-H7	SK7	BD Biosciences	560176
Mouse anti-human Vδ2	BD Horizon V421	B6	BD Biosciences	743749
Mouse anti-human TIM3 (CD366)	PE	7D3	BD Biosciences	563422
Mouse anti-human TIGIT	BB700	741182	BD Biosciences	747846
Mouse anti-human CD279 (PD-1)	APC-R718	EH12.1	BD Biosciences	566974
Mouse anti-human LAG-3 (CD223)	Alexa Fluor 647	T47-530	BD Biosciences	565716
Mouse anti-human CD27	PE-Cy7	M-T271	BD Biosciences	560609
Mouse anti-human CD45RA	BV605	5H9	BD Biosciences	740424
Mouse anti-human CD69	BV480	FN50	BD Biosciences	747519
Mouse anti-human TNF-α	APC	Mab11	BD Biosciences	551384
Mouse anti-human IFN-γ	BB700	B27	BD Biosciences	566394
Mouse anti-human CCR6	BB515	11A9	BD Biosciences	564479
Mouse anti-human CD25	PE	M-A251	BD Biosciences	555432
Mouse anti-human CD161	BB700	DX12	BD Biosciences	745791
Mouse anti-human CXCR3	PE-Cy7	1C6/CXCR3	BD Biosciences	560831
Rat anti-human CRTH2	Alexa Fluor 647	BM16	BD Biosciences	558042
Mouse anti-human CD127	APC-R718	HIL-7R-M21	BD Biosciences	566967
Mouse anti-human CCR7	BV421	2-L1-A	BD Biosciences	566743
Mouse anti-human CD4	V500	RPA-T4	BD Biosciences	560768
Mouse anti-human CD57	FITC	NK-1	BD Biosciences	555619
Mouse anti-human CD8	V500	SK1	BD Biosciences	561617
Mouse anti-human CD56	PE-Cy7	NCAM 16.2	BD Biosciences	335826
Mouse anti-human CD16	APC	3G8	BD Biosciences	561248
Mouse anti-human NKG2A (CD159a)	BV421	131411	BD Biosciences	747924
Mouse anti-human CD45	V500	HI30	BD Biosciences	560777
Mouse anti-human CD8	BV605	SK1	BD Biosciences	56416
Mouse anti-human CD16	FITC		BD Biosciences	555406
Mouse anti-human CD274 (PD-L1)	PE	MIH1	BD Biosciences	557924
Mouse anti-human CD39	BB700	TU66	BD Biosciences	745904
Mouse anti-human CD33	PE-Cy7	P67.6	BD Biosciences	333952
Mouse anti-human CD11b	APC	3G8	BD Biosciences	550019
Mouse anti-human IL-3Ralpha (CD123)	APC-R718	6H6	BD Biosciences	567287
Mouse anti-human CD14	APC-H7	MΦP9	BD Biosciences	560180
Mouse anti-human HLA-DR	V450	L243	BD Biosciences	655874
Mouse anti-human CD11c	BV480	B-ly6	BD Biosciences	566135
Mouse anti-human IFN-γ	BB700	B27	BD Biosciences	566394
Mouse anti-human TNF-α	APC	MAb11	BD Biosciences	551384
Mouse anti-human IL-17	PE	N49-653	BD Biosciences	560486
Mouse anti-human IL-10	APC-R700	JES3-19F1	BD Biosciences	567012
Mouse anti-human IL-4	PE-Cy7	8D4-8	BD Biosciences	560672

Reagents	Source	Cat. number
Stain Buffer (BSA)	BD Biosciences	554657
BD OneFlow™ PCD	BD Biosciences	659913
BD OneFlow™ Plasma Cell Screening Tube (PCST)	BD Biosciences	659912
Ionomycin calcium salt	Sigma-Aldrich	I0634
Phorbol 12-myristate 13-acetate (PMA)	Sigma-Aldrich	P8139
Monensin sodium salt	Sigma-Aldrich	M5273
Inside Stain Kit	Miltenyi Biotec	130-090-477
TCR γ/δ+ T Cell Isolation Kit Human	Miltenyi Biotec	130-092-892
OctoMACS™ Separator	Miltenyi Biotec	130-042-109
MS Column	Miltenyi Biotec	130-042-201
MACS® MultiStand	Miltenyi Biotec	130-042-303
Reagents for cell culture and isolation		
Reagent	**Source**	**Cat.number**
Ficoll-Paque PLUS	Cytiva	17144003
Dulbecco's Phosphate-buffered saline (DPBS) w/o calcium, w/o magnesium	Euroclone	ECB4004L
Daratumumab	MedChemExpress	HY-P9915
CountBright™ Absolute Counting Beads	Thermo Fisher Scientific	C36950
StableCel^{ITM} RPMI-1640 with stable glutamine and sodium bicarbonate	Sigma-Aldrich	R2405-500ML
HEPES buffer 1M	Euroclone	ECM0180
Penicillin-Streptomycin solution 100 X	Euroclone	ECB3001D
Heat-inactivated fetal bovine serum	Dominique Dutscher	S181H-500
TGF-β	Thermo Fisher Scientific	PHG9214
pH 8.0, RNase free	Thermo Fisher Scientific	AM9261
NH_4Cl	Millipore Sigma	A9434
$NaHCO_3$	Millipore Sigma	S5761
Bovine serum albumin (BSA)	Millipore Sigma	9430
HBSS without calcium, magnesium, phenol red	Euroclone	ECM0507
Luminex reagents		
Reagent	**Source**	**Cat.number**
Bio-Plex Pro Human Cytokine Screening 48-Plex Panel	Bio-Rad	12007283
Bio-Plex Calibration kit	Bio-Rad	171203060
Bio-Plex Validation kit 4.0	Bio-Rad	171203001
Bio-Plex Sheath fluid	Bio-Rad	171000055
Microbiota analysis		
Reagent	**Source**	**Cat.number**
QIAamp PowerFecal Pro DNA Kit	Qiagen	51804
Double-stranded DNA high-sensitivity assay kit	Invitrogen	Q32851

Other reagents, instruments and software	
BD FACSLyric™ Flow Cytometer	BD Biosciences
FlowJo software	Tree Star (version 10.5.3)
Infinicyt software	Cytognos (version 2.0.6)
R software	4.4.1

R studio	2024.09.0+375
NanoDrop 2000 Spectrophotometer	Thermo Scientific
Qubit 2.0 fluorometer	Invitrogen
MiSeq	Illumina
Bio-Plex 200 system	Bio-Rad
Tapestation	Agilent
High Sensitivity DNA ScreenTape	Agilent
NextSeq 550 system	Illumina

Integrated summary of results

This research comprehensively investigates key factors in MM pathogenesis and progression, including iron metabolism, immune cell profiles, cytokine signaling, gut microbiota, and the TME. It also explores novel biomarkers for risk stratification and treatment monitoring.

First, the study reveals that ferritin levels increase progressively from indolent to active gammopathies. Patients with low serum ferritin demonstrated significantly longer PFS during first-line treatment and OS. Moreover, ferritin levels correlates with systemic inflammation markers and a distinct BM immune microenvironment characterized by higher MM cell infiltration. Through bioinformatics analyses of large transcriptomic and single-cell datasets, the study identify a gene expression signature associated with ferritin biosynthesis, linking it to poorer outcomes, increased MM cell proliferation, and specific immune cell profiles (**see Part I**).

As MM evolves from MGUS and SMM to symptomatic disease, profound changes occur in the BM immune microenvironment. Advanced immune profiling tools, such as FlowCT, reveal significant alterations, including reductions in granulocytes and the granulocyte-to-lymphocyte ratio (GLR), alongside an increase in T lymphocytes.

Notably, baseline levels of BM granulocytes, granulocyte-to-lymphocyte, and granulocyte-to-T lymphocyte (GTL) ratios are associated with improved therapeutic outcomes, particularly in patients treated with Daratumumab-based regimens. Further analysis shows that autologous BM-derived granulocytes enhance Daratumumab-mediated cytotoxicity against neoplastic plasma cells, uncovering a novel granulocyte-dependent mechanism of action for Daratumumab in MM (**see Part II**).

The progression of MM is also marked by an increase in exhausted T cell phenotypes. Analysis of T cell exhaustion highlights the role of γδ T cells, which in MM patients exhibited elevated expression of exhaustion markers such as PD-1 and TIGIT, alongside reduced cytokine production. Functional assays demonstrate that co-culturing γδ T cells with MM cell lines replicates the altered phenotype observed in patients, suggesting that interactions within the TME drive this dysfunction (**see Part III**).

Furthermore, gut microbiota composition and cytokine signaling also play a critical role in MM progression. The study reveals a decline in microbial diversity as MM progresses from MGUS, suggesting that dysbiosis contributes to immune dysregulation and systemic inflammation, both of which promote tumor growth. Interestingly, specific pro-inflammatory cytokines are reduced in the plasma of MM patients, potentially slowing disease progression by limiting inflammation and

bone damage. However, the concurrent decrease in key antitumor cytokines fosters a permissive environment for tumor growth (**see Part IV**).

The final section of this study focuses on minimal residual disease (MRD) analysis, a cornerstone for evaluating treatment responses and predicting patient outcomes in MM. Distinct BM immune microenvironments were observed between MRD-positive and MRD-negative patients. MRD-negative patients exhibited a more balanced immune profile, characterized by reduced levels of immunosuppressive cell subsets and enhanced functionality of effector immune cells (**see Part V**).

Part I

Ferritin metabolism reflects MM microenvironment and predicts patient outcome

Ferritin, a protein responsible for storing and releasing iron, plays an important role in MM. Its levels are often elevated in patients with this condition, reflecting not only iron metabolism disturbances but also the disease's complex inflammatory and proliferative processes.

Despite high ferritin levels, the regulation of iron metabolism in MM is profoundly affected, leading to distinct and opposing consequences for different cellular processes. On one hand, iron is often sequestered and unavailable for erythropoiesis, contributing to the anemia seen in MM. On the other hand, while the normal erythron faces iron deficiency, the malignant plasma cells within the BM have a heightened demand for iron to fuel their uncontrolled growth. The ability of the cancerous clone to access and utilize iron is a critical factor that drives tumor proliferation and MM progression. This dual effect—iron deprivation contributing to anemia, and iron accessibility promoting malignancy—underscores the complex role of iron metabolism in MM, presenting potential therapeutic avenues aimed at disrupting iron supply to the tumor while managing anemia in affected patients (126).

Elevated ferritin levels may also serve as a prognostic marker in MM. Some studies suggest that higher ferritin concentrations could be associated with more aggressive disease and poorer outcomes, potentially linked to higher levels of inflammation and tumor burden (127–130).

This section of the project investigated the potential role of ferritin as a prognostic marker in patients with a new diagnosis of MM and its association with alterations in laboratory parameters and BM immune subpopulations. The stratification of patients based on ferritin levels revealed distinct immune cell compositions. Additionally, the bioinformatic analysis underscored the biological relevance of ferritin biosynthesis gene expression signatures, linking them to disease progression and patient prognosis (**see Appendix II**).

134 patients were included in the analysis, comprising 15 with MGUS, 17 with SMM, and 102 with MM, all with available serum ferritin levels at diagnosis. Patients with MM showed significantly higher mean serum ferritin levels than those with MGUS and SMM.

MM patients were stratified into low ferritin (LF) and high ferritin (HF) groups based on the median ferritin level. Survival analysis revealed that patients in the HF group had a worse median PFS than the LF group. Additionally, a systemic pro-inflammatory profile was observed in MM patients within the HF group. In detail, HF patients demonstrated elevated levels of creatinine, C-reactive protein, β2-microglobulin, as well as increased neutrophil-to-lymphocyte ratio and monocyte-to-lymphocyte ratio.

Principal component analysis (PCA) of laboratory variables across all MGUS, SMM, and MM patients revealed that LF patients clustered more closely with MGUS and SMM cases. This finding supports the notion that a non-inflammatory profile may be associated with a less aggressive form of disease. Additionally, patients with osteolytic bone lesions at diagnosis had significantly higher ferritin levels than those without, and ASCT-ineligible patients with low ferritin levels demonstrated better outcomes.

Moreover, the abundance of various immune cell populations was analyzed in BM aspirates from 25 patients (14 LF and 11 HF). MM patients in the HF group showed an increase in BMPCs, while other normal immune subpopulations, such as granulocytes and $CD38^{dim}$ NK cells, were significantly reduced.

A gene expression signature linked to ferritin biosynthesis was associated with poor outcomes, MM cell proliferation, and distinct immune cell profiles, as shown through bioinformatic analyses of large transcriptomic and single-cell datasets. Analysis of 859 baseline transcriptomes from the MMRF CoMMpass study identified six patient subclusters, with three ferritin-enriched clusters showing high FTL (Ferritin Light Chain 1) and FTH1 (Ferritin Heavy Chain 1) expression, classified as the HF group. One cluster (C5), characterized by high cell proliferation and S-phase gene overexpression, had significantly worse survival. Single-cell data revealed that patients with elevated FTH1 or FTL1 levels had fewer NK cells, CD4 naïve T cells, and B cells, but more monocytes, indicating ferritin's impact on immune composition.

These findings emphasize the need for further exploration of ferritin as both a biomarker and potential therapeutic target in MM, with implications for personalized treatment strategies and improved patient management.

Part II

FlowCT analysis reveal distinct immune profile along MM evolution

Given the frequent overlap in the genomic profiles of preneoplastic conditions with that of active MM, it is imperative to pinpoint the key mechanisms driving the transition from these early stages to full-blown malignancy. These critical drivers may not solely reside within the malignant plasma cells themselves but could also originate from the surrounding TME. In this context, the immune system emerges as a central player, exerting either protective or promoting effects on disease progression.

A deeper understanding of how the immune system contributes to the progression from MGUS or SMM to active MM has profound clinical implications. First and foremost, it could enhance the ability to stratify patients based on their risk of progression. By profiling immune cell composition, function, and signaling within the BM, high-risk individuals who are more likely to develop symptomatic MM could potentially be identified. This would enable more tailored monitoring strategies and preventive measures, ensuring that high-risk patients receive closer follow-up and earlier intervention, while sparing low-risk individuals from unnecessary treatments.

Furthermore, this approach could lead to the identification of valuable biomarkers that serve not only as predictors of disease progression but also as indicators of treatment response. By establishing a clearer correlation between these biomarkers and therapeutic outcomes, clinicians could make more informed decisions regarding treatment strategies. This would enable more precise monitoring of patients, allowing for timely adjustments to therapy based on their individual responses. Ultimately, such advancements could enhance personalized medicine, improving overall patient care and outcomes.

In this context, this section of the project focused on mapping changes in peripheral blood and BM immune cell composition throughout the MGUS-to-MM progression. Additionally, the composition of the BM immune compartment was analyzed in relation to clinical outcomes, aiming to identify specific cell types associated with better therapeutic responses in MM patients.

FlowCT, a semi-automated workflow designed for the deconvolution of immunophenotypic data and objective analysis of large datasets (115), was used to assess BM immune populations in 9 MGUS, 14 SMM, and 127 MM patients. The analysis revealed substantial differences in immune cell composition between the pre-malignant stages and active MM, underscoring the evolving nature of the BM microenvironment as the disease advances.

The transition to active MM coincided with a decline in granulocyte levels and a rise in T lymphocytes. This resulted in a decline in both the granulocyte-to-lymphocyte (GLR) and to-T lymphocyte (GTL) ratios in bone marrow. Notably, MM patients exhibited a reduction in effector/terminally differentiated ($CD27^-$) T lymphocytes/NK cells. Delving into the influence of these immune cell populations on MM patient's outcome, here was observed that a higher baseline percentage of BM granulocytes and elevated GLR and GTL ratio correlate with an improved PFS. Notably, the influence of these pre-treatment immune patterns on patient' outcome is particularly pronounced in those undergoing Daratumumab-based regimen. Additionally, the comprehension of Daratumumab's anti-MM activity was enhanced by introducing a novel mechanism mediated by BM-derived granulocytes. Specifically, autologous BM-derived granulocytes augment Daratumumab-mediated cytotoxicity against neoplastic plasma cells, significantly increasing the anti-tumor activity of BMMCs alone (**see Appendix III**).

Contextually, a comprehensive analysis of immune composition, including myeloid and lymphoid subpopulations of T cells, B cells, and NK cells, along with the distribution of immune checkpoints, was conducted in both BM and peripheral blood samples from these patients.

In MM patients, there was a marked decrease in circulating naïve $TIGIT^+$ CD8 T cells, with mean percentages declining from 12.4% in MGUS to 4.16% in MM ($p<0.05$). However, the percentage of this immune subset is higher in BM of MM patients compared to blood (4.16% vs 8.60%; respectively) (**Figure 3C**).

Similarly, the proportion of circulating naïve $TIGIT^+$ $TIM3^+$ CD8 T cells also decreased significantly, from 2.18% in MGUS to 1.24% in SMM and 1.17% in MM ($p<0.01$). The BM counterpart was reduced in SMM patients compared to those with MGUS (1% vs 4%; respectively) (**Figure 3C**).

In contrast, a notable increase in circulating TEMRA T cells was observed, particularly among $CD57^+$ cells. The mean percentages of these cells were significantly higher in the progression from MGUS to SMM and then to active MM, with values of 7.5% for MGUS, 20.1% for SMM, and 21.6% for MM ($p<0.01$). Among the CD4 T cell subsets, there was a reduction in the BM $CCR6^+$ $CD161^+$ memory subset, with mean percentages falling from 7.07% in MGUS to 4.54% in SMM and further to 3.72% in MM ($p<0.05$) (**Figure 3C**). Conversely, there was a significant increase in IL-17-producing CD4 T cells within the BM with levels rising from 6.7% in MGUS to 22% in MM ($p < 0.05$) (**Figure 3D**). No significant variations were found after *in vitro* stimulation with ionomycin and PMA. The elevation of IL-17-producing T cells may indicate a shift in the immune response that could contribute to inflammatory processes associated with disease progression.

Additionally, the population of non-classical monocytes expressing HLA-DR and CD11c showed a decline as the disease progressed in peripheral blood and BM (mean, 7% MGUS vs 10% SMM vs

3,7% MM for peripheral blood, and 4.53% MGUS vs 4.93% SMM vs 2.45% MM for BM) ($p<0.05$) (**Figure 3C**).

Overall, these findings highlight significant alterations in the immune cell composition and function during the progression from MGUS to MM.

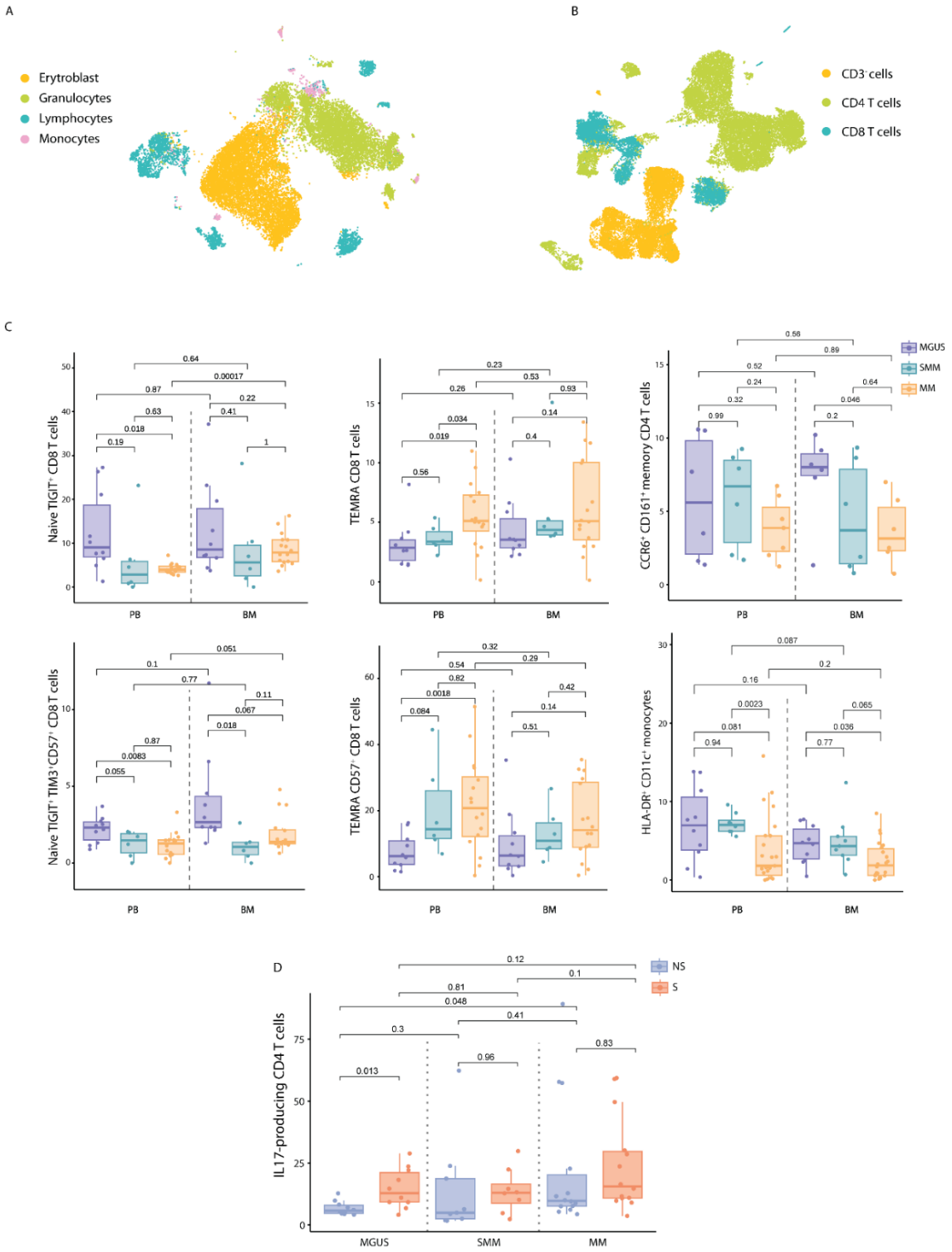

Figure 3. The transition from MGUS-to-MM involves notable changes in immune cell subsets
UMAPs of identified major bone marrow immune cells (A) and lymphocyte subsets (B). (C) Boxplots showing a statistically different distribution of lymphocyte and monocyte populations between MGUS, SMM, and MM patients. (D) Boxplot showing IL17-producing CD4 T cells between MGUS, SMM, and MM patients.

Part III

Examining γδ T cell responses in multiple myeloma evolution: a study of immunological functionality and exhaustion

Unconventional γδ T cells play a vital role in connecting the innate and adaptive immune responses and constitute approximately 1-10% of the total $CD3^+$ T lymphocyte population. They exhibit distinct phenotypic and functional characteristics compared to conventional αβ T cells, particularly in the unique structural organization of their T cell receptor (TCR), consisting of one γ and one δ chain. Unlike αβ T cells, the γδ TCR can recognize antigens independently of MHC restriction, enabling these cells to identify a wide variety of ligands, including unconventional MHC-related molecules and non-MHC-related self-proteins (131,132).

In humans, the primary subsets of γδ T cells, classified based on the expression of the δ chain of the TCR, are Vδ1 and Vδ2 (133). Vδ1 T cells represent the predominant subset of γδ T cells at birth and are mainly localized in tissues and mucosal surfaces, especially within the epithelium of the gastrointestinal, respiratory, and urogenital tracts. These cells are adept at recognizing stress-related antigens, such as MHC class I-related molecules A and B (MICA/MICB) and UL16-binding proteins, which are expressed by transformed or malignant cells, as well as glycolipids presented by CD1b, CD1c, and CD1d molecules.

On the other hand, the Vδ2 subset comprises 50-75% of the total γδ T cells and is typically associated with the γ9 chain, commonly referred to as Vγ9Vδ2. This subset is predominantly found in peripheral blood. Vδ2 T cells are activated and expanded in response to both endogenous and exogenous phosphoantigens, such as isopentenyl pyrophosphate (IPP) and those derived from the 1-deoxy-D-xylulose-5-phosphate pathway, including (E)-4-hydroxy-3-methyl-but-2-enyl pyrophosphate (HMBPP) (134).

Costimulatory receptors, inhibitory receptors, and lymphokines finely regulate their functions. A significant proportion of γδ T cells express a variety of activating and inhibitory NK receptors, including natural cytotoxicity receptors (NCRs) such as NKp30 and NKp44, as well as lectin-like receptors (NKG2A/C/D) and immunoglobulin-like receptors (both activating and inhibitory KIRs). Moreover, γδ T cells can differentiate into various T helper-like subtypes, including Th1, Th2, Th9, and Th17. This differentiation allows them to produce a broad spectrum of cytokines that facilitate their diverse physiological functions (135,136).

By integrating the functionality of a TCR with a diverse array of natural cytotoxicity receptors and their ability to produce essential immune molecules such as IFN-γ, granzyme, and perforin, these cells can effectively orchestrate a wide range of immune responses (136). Their multifunctionality allows them to play critical roles in various physiological and pathological processes (**Figure 4,5**).

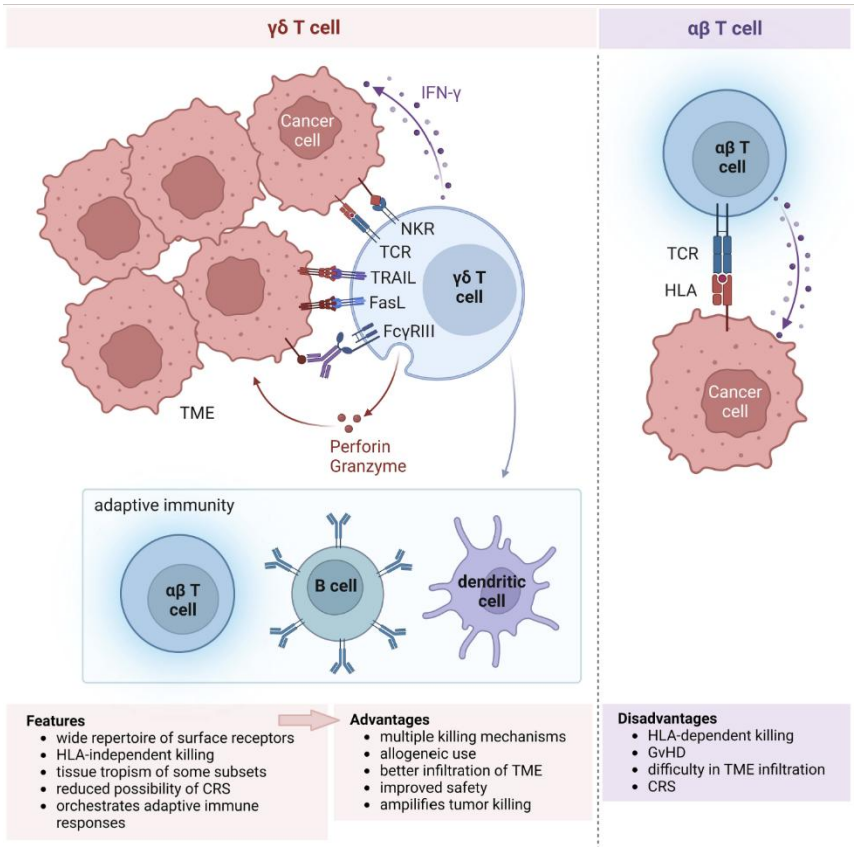

Figure 4. Comparison of key characteristics and functional properties of γδ T cells versus αβ T cells
Wang CQ et al. Front Immunol. 2024 (137)

Evidence indicates that γδ T cells play a pivotal role in immune surveillance, exerting cytotoxicity and influencing immunomodulation through cytokines within the complex TME. Contextually, γδ T cells exhibit characteristics associated with immune suppression rather than tumor control. Indeed, they may become polarized or influenced by the TME to promote tumor growth and immune evasion (136–138).

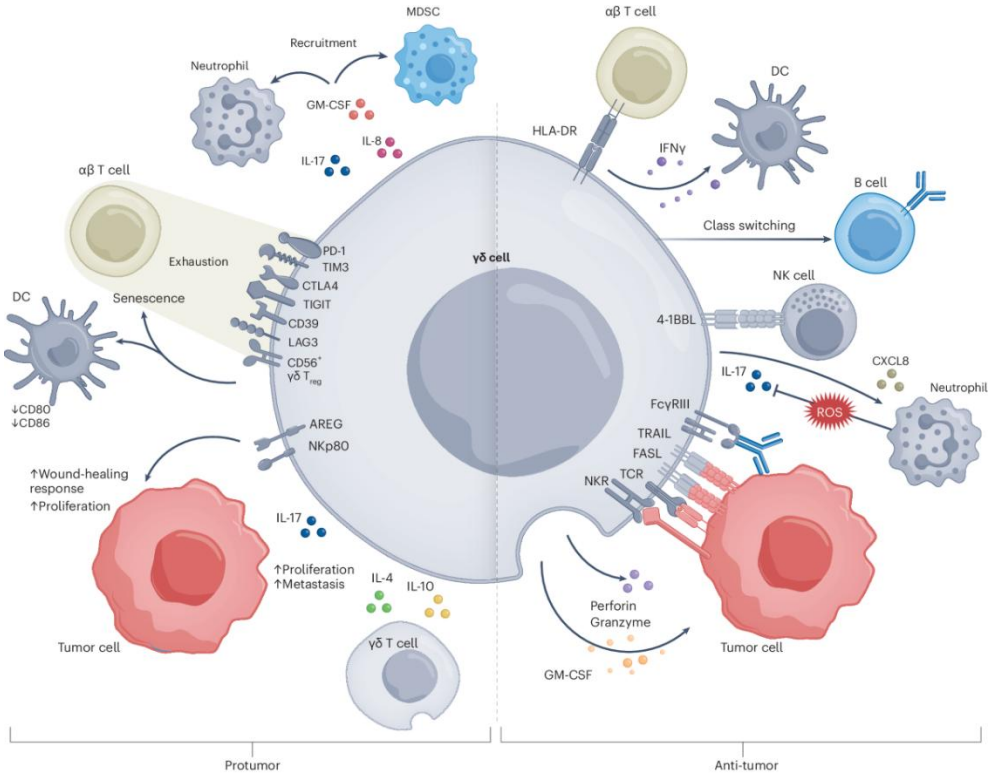

Figure 5. Protumoral and anti-tumoral roles of γδ T cells
Arias-Badia M. et al. Nat Cancer (2024) (136)

Gentles et al. (139) described γδ T cells as components of the leukocyte composition in bulk tumor transcriptomes of hematological disorders, including MM. However, the precise nature of their involvement in MM and precursor conditions is still under investigation, highlighting the necessity for a comprehensive understanding of their functions and potential therapeutic applications.

In this section of the project, flow cytometry and single-cell analysis were conducted to explore the role of γδ T cells in the immunopathogenesis of MM and its precursor stages. This investigation focused on assessing their functionality and understanding how the TME influences their behavior and activity (**see Appendix IV**).

We performed scRNA-seq on BM samples from patients with MGUS (n=3), SMM (n=5), and MM (n=10), along with HD (n=4). After quality control, we obtained transcriptional data from an average of 4,373 γδ T cells, isolated from 167,297 cells. An unsupervised clustering analysis identified eight distinct γδ T cell clusters. Two clusters resembled naïve cells, while the others were either enriched with cytotoxic markers or represented activated effector memory cells. No significant differences in cluster proportions were found across disease stages. A pseudo-bulk analysis revealed that the expression of *HAVCR2*, encoding the immune checkpoint protein TIM3, was significantly higher in MM patients than in preneoplastic stages and HD.

To validate these transcriptomic findings, the main subsets of γδ T cells, named Vδ1 and Vδ2, were analyzed using flow cytometry in peripheral blood and BM samples from patients with MGUS

(n=13), SMM (n=11), and MM (n=35), as well as from HD (n=11). No significant differences in the frequencies of both circulating and BM Vδ1 and Vδ2 T cells were found throughout disease progression. Notably, a significant increase in effector memory Vδ2 T cells ($CD45RA^{-}$ $CD27^{-}$) was observed in patients with MM, accompanied by an upregulation of exhaustion markers such as TIM3 and PD1. This suggests a functional compromise of these cells, which was further corroborated by *in vitro* stimulation assays demonstrating reduced cytokine production (TNF-α and IFN-γ) in γδ T cells of MM patients. Co-culture experiments with MM cell lines indicated that direct interaction with malignant cells drives the differentiation of γδ T cells towards an effector memory and exhausted phenotype, characterized by increased TIM3 expression.

Patients with varying levels of TIM3 expression on γδ T cells exhibited significant differences in clinical and immunological profiles, suggesting a potential link between TIM3 expression and disease progression in MM. Specifically, lower TIM3 expression was associated with elevated lactate dehydrogenase (LDH) levels ($p<0.05$) and a predominance of clonal plasma cells co-expressing CD81 and CD117, indicating a more aggressive disease phenotype and highlighting the role of TIM3 in shaping the immune microenvironment in MM.

Finally, we analyzed the relationship between γδ T cells and clinical outcomes in MM by examining PFS in patients based on various γδ T cell populations in the BM. Our findings revealed that higher levels of $PD1^{+}$ Vδ2 T cells present in the BM, as well as effector memory Vδ2 T cells, correlated with shorter PFS, indicating their significance as prognostic factors in MM.

These findings underscore the impairment of γδ T cells as MM progresses, evidenced by their shift toward an exhausted and effector memory phenotype with reduced functionality. This suggests a key role for γδ T cells in MM's immune evasion mechanisms. Moreover, circulating γδ T cells appear to mirror the BM microenvironment, indicating their potential as a less invasive tool for monitoring disease progression and predicting outcomes in patients with monoclonal gammopathies. Given its overexpression, targeting TIM3 represents a promising strategy to restore γδ T cell function and enhance patient response. The correlation between TIM3 expression and disease progression further supports its potential as a biomarker for patient stratification, identifying those who may benefit from TIM3-targeted therapies, especially in combination with agents that enhance γδ T cell activation.

Part IV

Disease progression tied to changes in cytokine, chemokine, and microbiota profiles

Cytokines and chemokines play a crucial role in regulating immune responses, and their altered expression along disease progression provides insight into the mechanisms underlying immune escape and tumor growth (140). This section of the project investigates the levels of key cytokines and chemokines using Luminex assays in both BM and peripheral blood samples from 12 MGUS, 12 SMM, and 12 MM patients, highlighting another face of immune alterations that occur throughout disease progression and their potential implications. This evaluation demonstrated a significant reduction in several key immune mediators in patients with MM. Specifically, the observed decrease in levels of GM-CSF, IFN-α2, IFN-γ, IL-1β, IL-2, IL-2Rα, IL-3, IL-10, IL-13, LIF, and MCP-1/CCL2 suggests impaired T cell activation and functionality, diminished immune cell infiltration, and a weakened inflammatory response. (**Figure 6B**).

Moreover, the analysis of plasma samples from peripheral blood of MM patients showed a notable decrease in MIP-1α, PDGF-BB, IL-16, IL-1β, IL-4, IFN-α2, IL-13, IL-8, IL-2, IL-10, LIF, MIG, IFN-γ, MCP-1, and IL-2Rα levels when compared to individuals with preneoplastic conditions, and HD (**Figure 7**). Many of these cytokines are crucial for the activation and the chemotaxis of T and NK cells; their reduction reflects a compromise in immune surveillance, alterations in the tumor microenvironment, and increased permissiveness for the growth of myeloma cells. This notable reduction in immune mediators underscores the systemic immune dysregulation commonly associated with MM, suggesting that the disease may promote alterations in immune function that facilitate tumor survival and progression.

Interestingly, this immune impairment is not limited to MM but is also detectable in MGUS and SMM patients, when compared to HD. In patients with SMM, the levels of key cytokines, including PDGF-BB, IL-1RA, IL-1β, IL-16, IL-1Rα, IFN-α2, IL-13, LIF, IFN-γ, and IL-18, were found to be significantly reduced compared to HD (**Figure 7**). Reducing these cytokines may have a complex and dual effect on disease progression. A decrease in specific pro-inflammatory cytokines, such as IL-1β and IL-1RA, could lead to a slower rate of bone destruction and a reduction in inflammatory processes, thereby delaying the onset of symptomatic disease. This attenuation of inflammation might create a more stable microenvironment in which the malignant plasma cells have less support for their growth and survival. Conversely, reducing important antitumor cytokines, including IFN-γ, IFN-α2, and IL-18, could significantly impair immune surveillance. These cytokines are crucial for activating immune cells, such as T cells and NK cells, which play a vital role in identifying and eliminating malignant cells. A decrease in their levels may create an environment conducive to tumor growth, as the immune system becomes less capable of recognizing and

targeting the emerging tumor cells. As a result, this immunosuppressive shift could accelerate the progression from SMM to active MM, allowing for more aggressive disease features to develop.
Additionally, IP-10 (CXCL10), a chemokine critical for the recruitment of immune cells, was lower in SMM patients than those with MGUS, suggesting distinct variations in immune activation between these plasma cell disorders. No significant differences were found for the other cytokines and chemokines for both samples (**Figure 8,9**).
In summary, while reducing certain pro-inflammatory cytokines may temporarily slow disease progression by limiting inflammation and bone damage, the simultaneous decrease of key antitumor cytokines could foster a permissive environment for tumor growth. This interplay underscores the complexity of cytokine dynamics in MM progression and highlights the importance of understanding these mechanisms in developing effective therapeutic strategies.

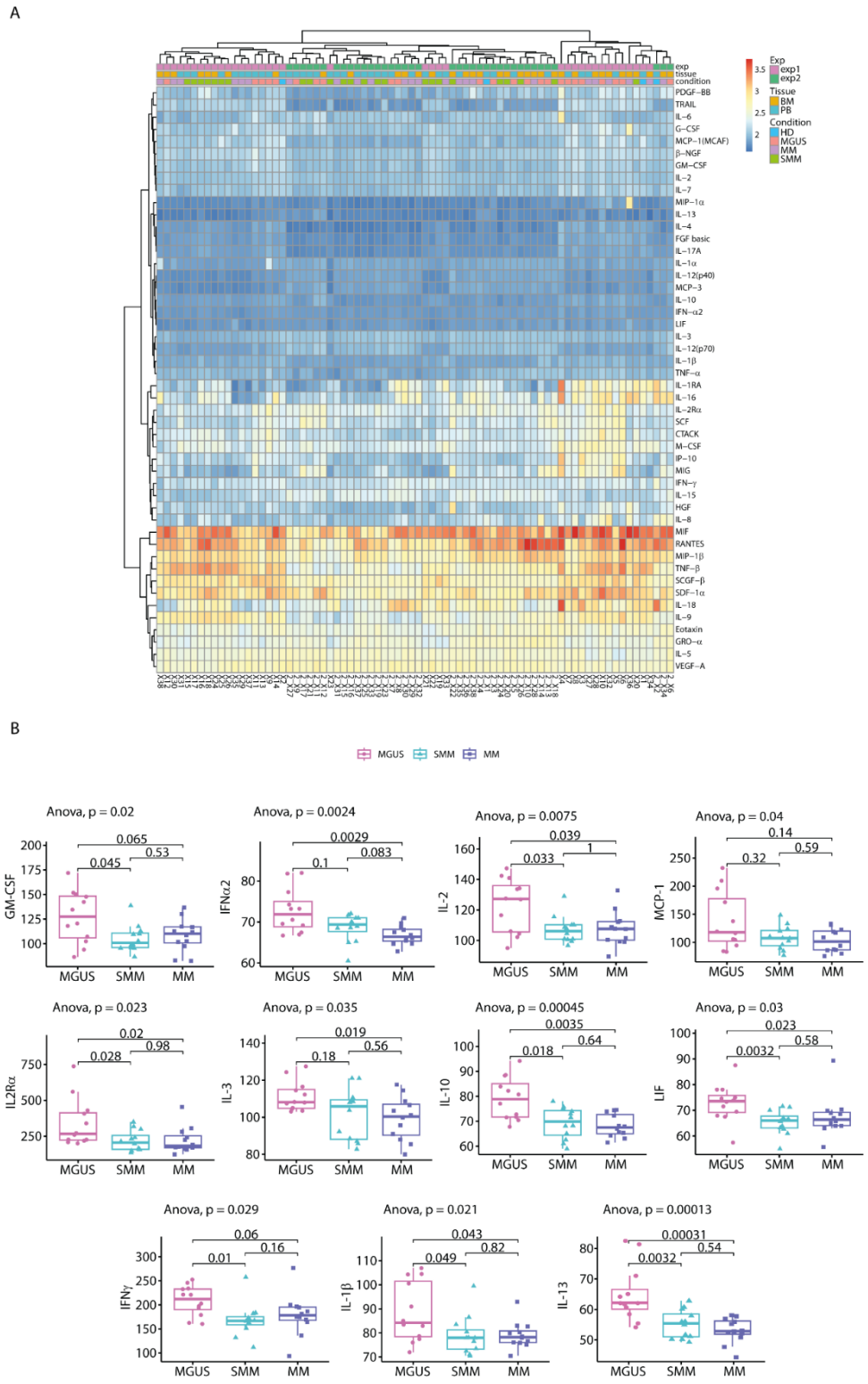

Figure 6. Shifts in BM cytokine and chemokine profiles are characteristic of the progression of MM
(A) The heatmap displays the expression levels of variables (rows) across different samples (columns). The column annotations include three key characteristics: clinical condition (HD, MGUS, SMM, MM), tissue type, and experiment number (1 or 2). These annotations are represented by colored bars above the heatmap, with distinct colors for each category. The color scale in the heatmap reflects the variation in logarithmic values, highlighting differences in expression profiles between clinical conditions and tissue types analyzed. Hierarchical clustering shows relationships between cytokines/chemokines and disease progression (B) Boxplots illustrating the significant differences in the levels of various

cytokines and chemokines in plasma samples collected from BM along MM evolution. All values are expressed in mean-fluorescence intensity (MFI). Abbreviations: PB, Peripheral blood; BM, bone marrow; exp, experiment.

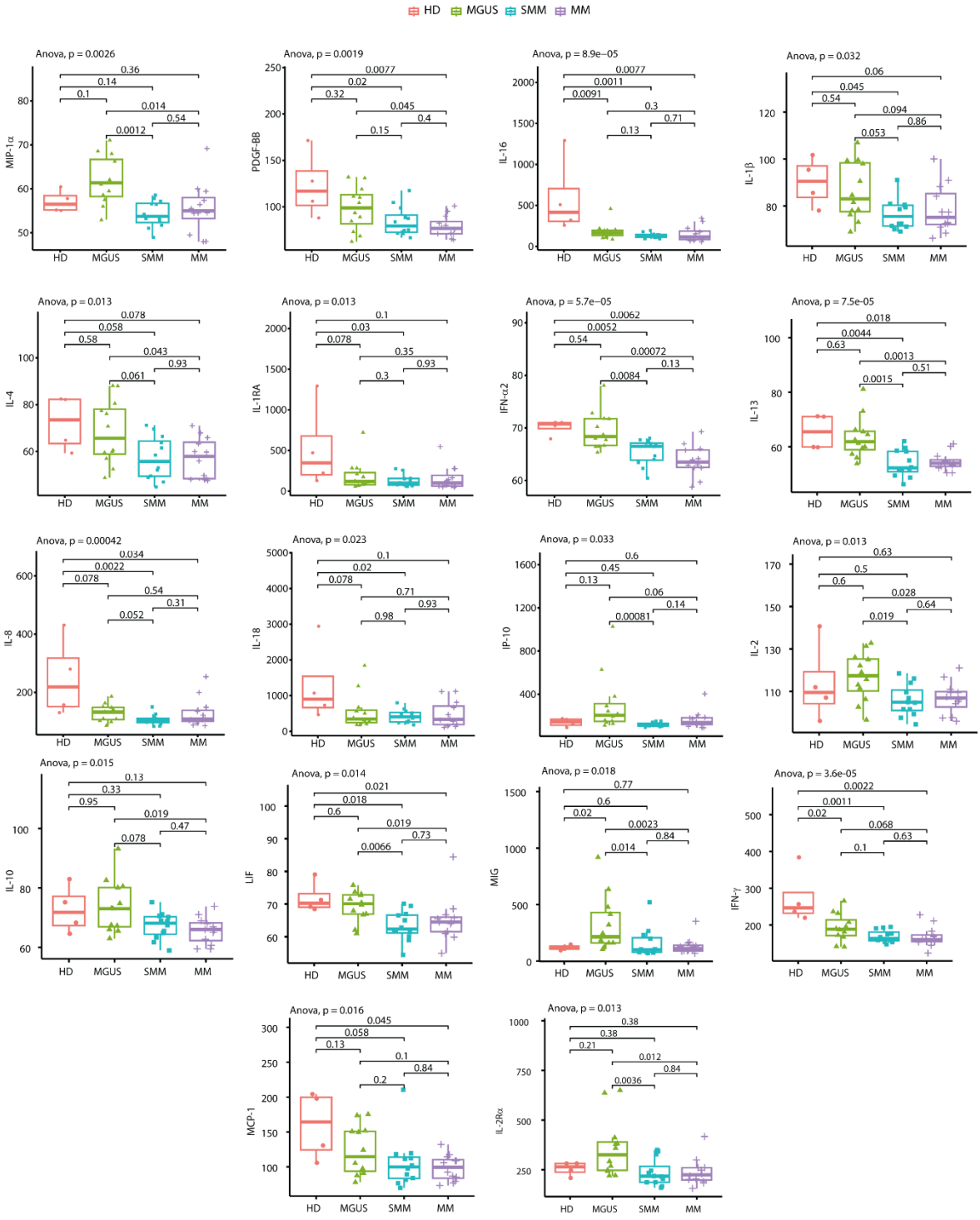

Figure 7. Shifts in peripheral blood cytokine and chemokine profiles are characteristic of the progression of MM
Boxplots illustrating the significant differences in the levels of various cytokines and chemokines in plasma samples collected from peripheral blood along MM evolution. All values are expressed in mean-fluorescence intensity (MFI).

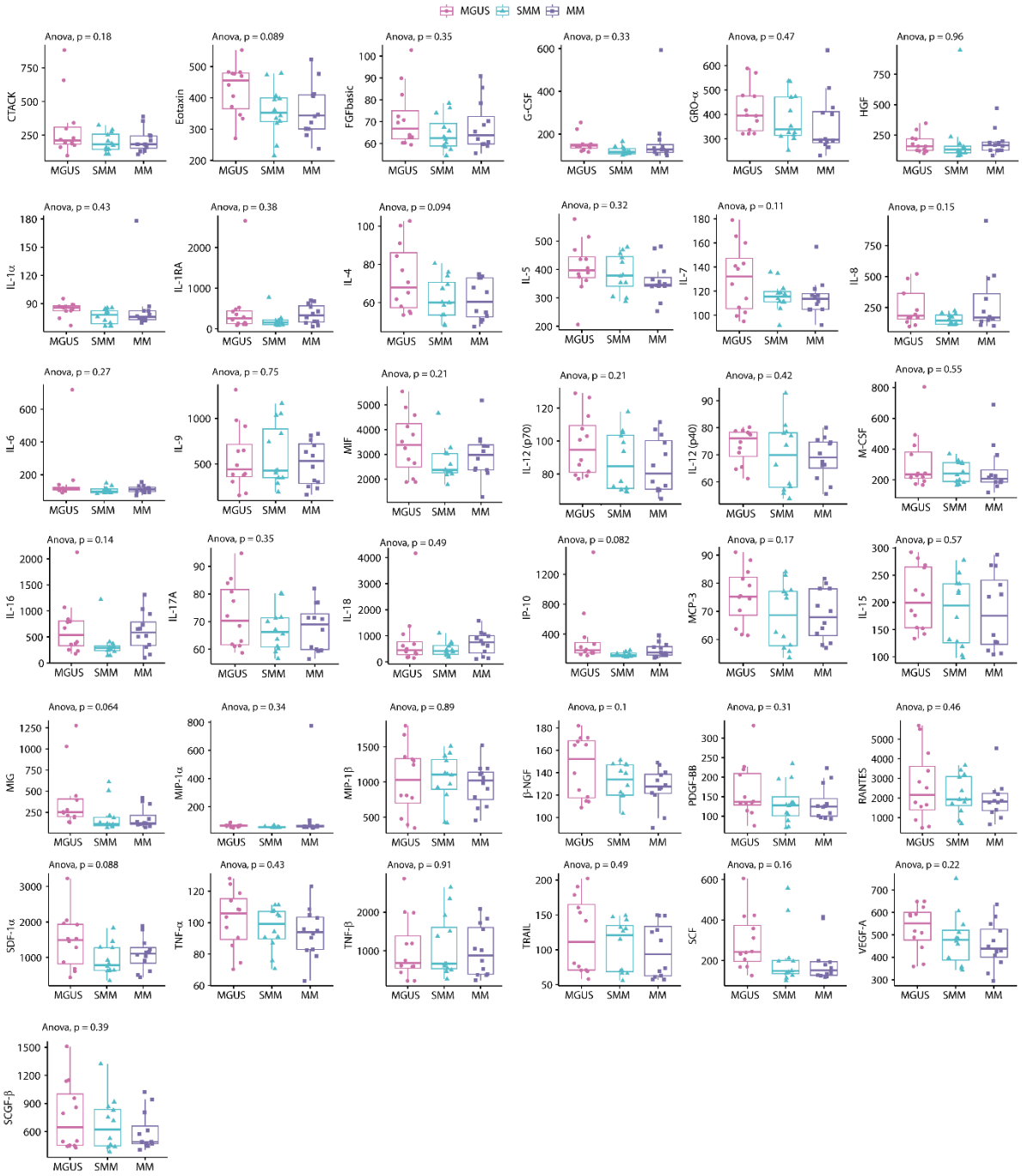

Figure 8. Comparison of cytokine and chemokine levels in BM plasma samples during MM progression
Boxplots illustrating the non-significant differences in the levels of various cytokines and chemokines in plasma samples collected from BM along MM evolution. All values are expressed in mean-fluorescence intensity (MFI).

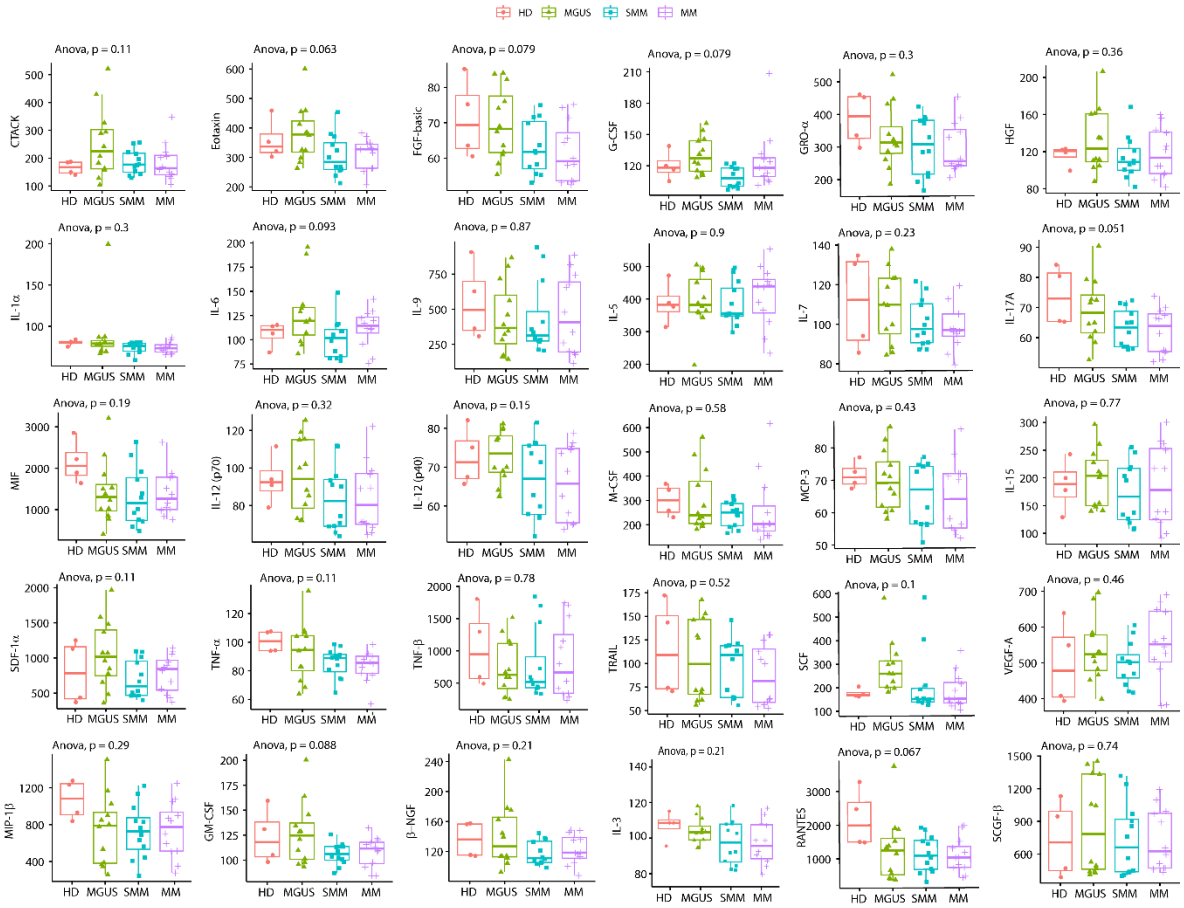

Figure 9. Comparison of cytokine and chemokine levels in PB plasma samples during MM progression
Boxplots illustrating the non-significant differences in the levels of various cytokines and chemokines in plasma samples collected from PB along MM evolution. All values are expressed in mean-fluorescence intensity (MFI). Abbreviations: PB, peripheral blood.

In addition to immune alterations, recent findings reveal significant metagenomic changes in the composition of commensal bacteria and an increased colonization by opportunistic bacteria as the disease progresses from precursor conditions to active myeloma (141–144). These microbiota alterations may worsen immune dysregulation, inflammation, and tumor progression. The changes observed in the microbiota throughout the spectrum of MM could serve as prognostic indicators for assessing the risk of transformation from MGUS to active disease and provide promising opportunities for innovative interventions aimed at modifying the gut environment to improve patient outcomes. Furthermore, numerous clinical and preclinical studies have underscored the influence of the gut microbiota on the therapeutic responses of MM patients (145).

In this section of the project, microbiota composition was evaluated during MM progression. Fecal samples from 41 patients were analyzed, including 10 with MGUS, 15 with SMM, and 16 with MM.

Alpha diversity analysis was first performed, utilizing rarefaction based on sampling technique to account for the effect of sample size on observed species units. The rarefaction curves indicated that as the number of reads increased, diversity stabilized across all samples, demonstrating sufficient sequencing depth to capture most species. While individual sample differences were noted in the first panel (**Figure 10A**), the group-level analysis (second and third panels) showed nearly identical curves across the three clinical states, suggesting no significant differences in species richness between groups. The overlapping confidence bands in the third panel further supported this observation.

Next, alpha diversity was evaluated to assess species richness and evenness within specific microbial communities. **Figure 10B** illustrates the distribution of various alpha diversity indices (Observed, Chao1, ACE, Shannon, Simpson, and Pielou) across the three groups, while **Figure 10C** shows these indices for individual samples. The analysis revealed similar levels of microbial diversity across the clinical conditions, as indicated by p-values close to or above 0.05 (**Figure 10B**). The bar plots provided a more detailed view of how alpha diversity indices varied within each group, highlighting significant within-group variability and indicating that microbial diversity can differ considerably between individual samples, even within the same clinical group (**Figure 10C**). This pattern persisted when the MGUS and SMM groups were combined into a "No MM" category (**Figures 10D, E**).

The analysis of bacterial phyla, orders, and families across the clinical groups MGUS, SMM, and MM revealed progressive shifts in gut microbiota composition, which may be linked to the progression of MM. From phylum to family levels, increasing complexity and variation in bacterial abundances were observed between the groups, both in terms of relative and rarefied abundance (**Figures 11A,C**). Relative abundance provided a proportional view of various bacteria without adjusting for sample size, offering insight into the microbiota composition of each patient. However, it did not account for differences in sample sizes. In contrast, rarefied abundance normalized bacterial counts based on sample size, allowing for more accurate comparisons across clinical groups. These rarefied values demonstrated that while certain bacterial species may appear in similar proportions, their actual quantities can vary significantly between MGUS, SMM, and MM.

MGUS is characterized by a more balanced microbiota, resembling that of healthy individuals, with a higher abundance of beneficial phyla such as *Bacteroidota* and *Actinobacteriota* (**Figure 11A**), as well as beneficial orders and families like *Lachnospirales*, *Oscillospirales*, *Bacteroidales*, *Lachnospiraceae*, and *Bifidobacteriaceae* (**Figures 11B, C**).

This suggests that MGUS patients maintain a healthier gut environment, while SMM represents an intermediate stage, showing gradual shifts towards dysbiosis with reductions in some beneficial bacteria, although less pronounced than in MM. In MM, significant dysbiosis is evident, with

marked decreases in beneficial phyla, orders, and families like *Actinobacteriota* and *Verrucomicrobiota*, alongside increases in potentially pathogenic groups such as *Proteobacteria*, *Enterobacterales*, *Enterobacteriaceae*, and *Streptococcaceae*. This imbalance may contribute to heightened inflammation, reduced production of beneficial metabolites, and compromised gut health.

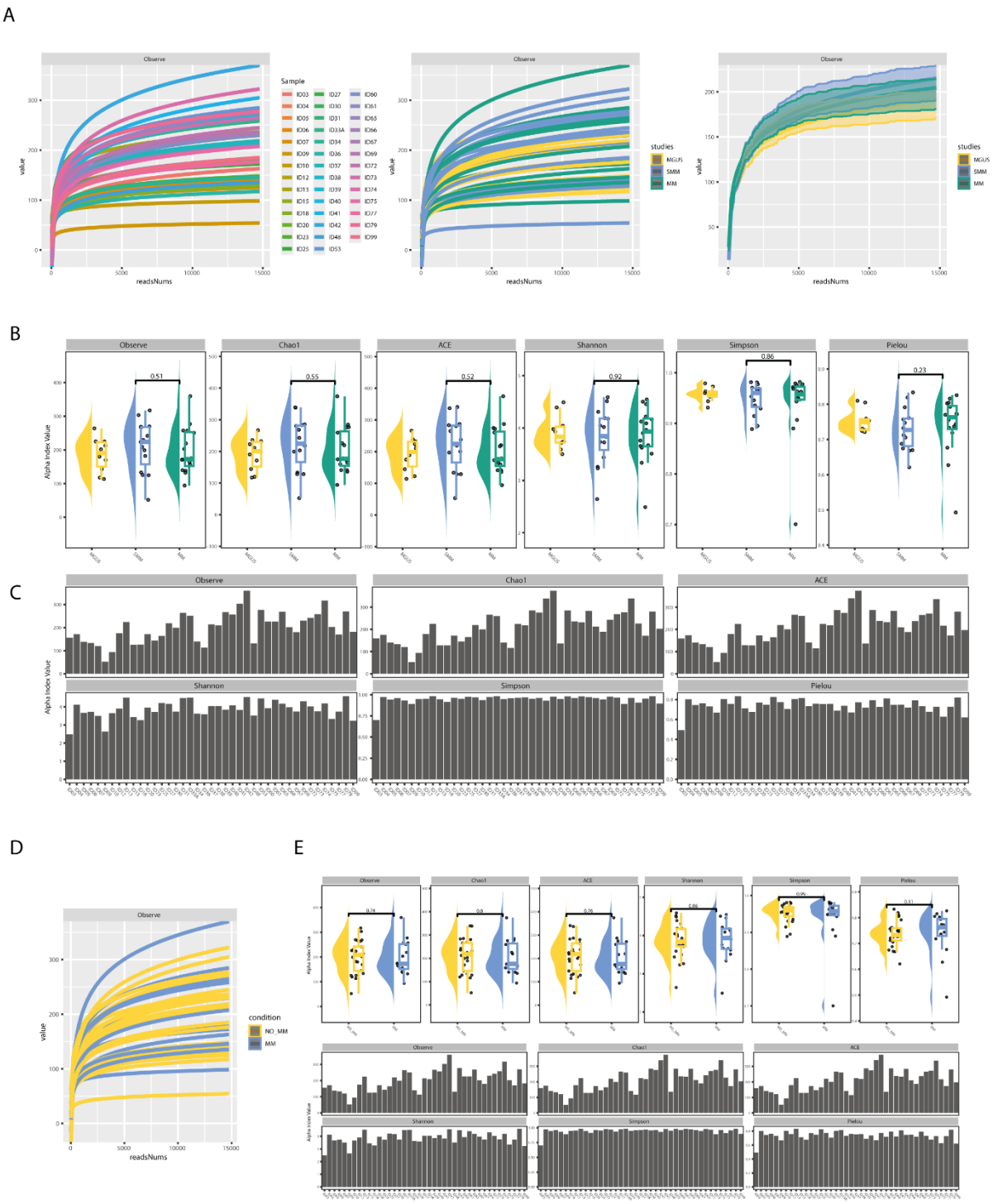

Figure 10. Comparative analysis of alpha diversity indices in microbial communities along MM progression
(A) The rarefaction curves are organized by individual samples (left panel), clinical status (center panel) and including confidence bands, which likely indicate variability within each group (right panel). In the left panel the curves illustrate the increase in observed diversity ("Observed") as the number of sequenced reads increases. With a sufficient number of reads, the curves tend to stabilize, indicating that most of the diversity has been captured for each sample. The variety of curves suggests that some samples exhibit greater species richness (higher curves), while others show less (lower curves). In the center panel the relationship between the number of reads and the number of observed species is highlighted. The curves from the different groups tend to overlap, suggesting that visually, the three groups do not show substantial differences in species richness. In the right panel the colored bands highlight the range of diversity variation for the MGUS, SMM, and MM groups. (B) The violin plots display the distribution of alpha diversity indices across the MGUS, SMM, and MM groups. Each panel corresponds to a different diversity index. (C) The bar graphs depict the distribution of alpha diversity indices for each individual sample. (D-E) Similar analysis was conducted for non-MM and MM groups.

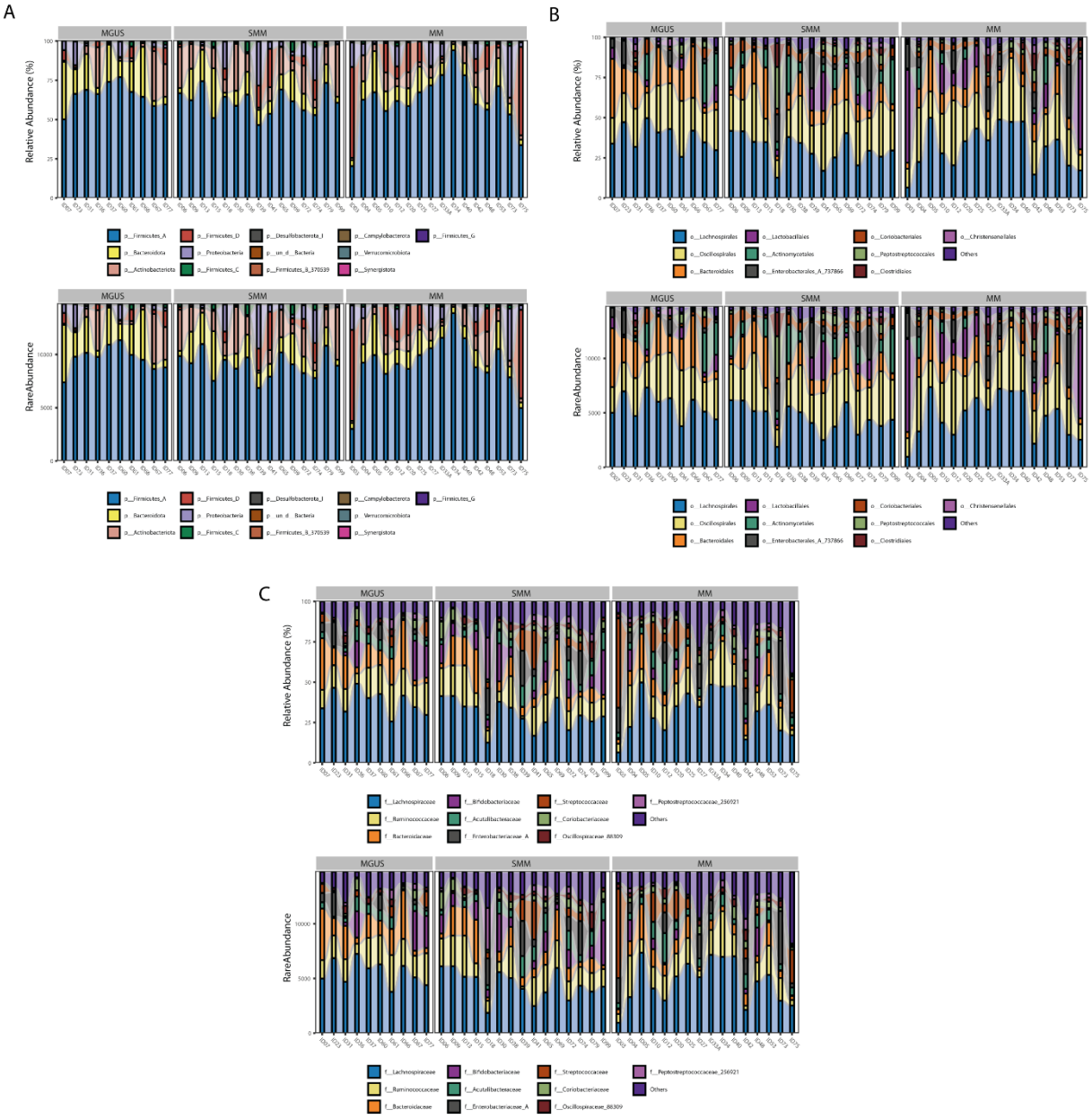

Figure 11. Bacterial composition by phyla, orders, and families along MM progression
The figure displays bacterial composition at three taxonomic levels: phylum (A), order (B), and family (C). In the relative abundance chart, the y-axis represents relative abundance as a percentage, while the x-axis organizes the samples into three primary groups (MGUS, SMM, MM). Different colored bars indicate the major bacterial phyla. In the rarefied abundance chart, the y-axis shows rarefied abundance, expressed as a numerical value for each bacterial group. The x-axis structure mirrors that of the previous chart, with samples grouped in the same way. This visualization method accounts for sample size variations, enabling a more accurate comparison between groups.

Beta diversity was subsequently assessed. While alpha diversity evaluates species diversity within a single sample, beta diversity—calculated using Bray-Curtis distance and represented on the y-axis—reflects the dissimilarity in microbial composition between samples from different patient groups (**Figure 12A**). Higher values indicate greater differences in microbial composition among the groups. The comparisons between patients with MGUS and MM, SMM and MM, as well as MGUS and SMM, revealed significant differences in microbial diversity ($p=0.00064$, $p=0.0001$, $p=0.0075$, respectively). These findings suggest that notable changes occur in microbiome composition as patients progress from MGUS (early stage) to SMM (intermediate stage) to MM. Conversely, comparisons within the same group, such as "MGUS vs. MGUS," "MM vs. MM," and "SMM vs. SMM," did not show significant differences, as anticipated. This confirms the significant differences observed between distinct disease stages (**Figure 12A**).

Moreover, principal coordinates analysis (PCoA) and the Shannon Index were used to assess microbial diversity and group similarities (**Figure 12B**). PCoA illustrates the distance or similarity between samples from different clinical groups, while the Shannon Index measures community diversity. Higher Shannon values (between 4.0 and 4.5) reflect greater microbial diversity, typically associated with healthier conditions or earlier disease stages where diversity is better preserved. In contrast, lower Shannon values (between 2.5 and 3.0) suggest reduced diversity, often seen in advanced disease stages. Lower diversity is usually linked to a microbial community dominated by a few species, likely due to pathological changes such as chronic inflammation or immune dysfunction.

The analysis revealed significant differences between MGUS, SMM, and MM. The distinct separation between MGUS and MM indicates that marked changes in microbial composition accompany the transition from asymptomatic to advanced disease. However, the PCoA axes (PCo1 and PCo2) explained 10.81% and 6.5% of the variance, respectively, accounting for about 17% of the total variability (**Figure 12B**). This suggests that while these components capture some differences between groups, other factors likely contribute to the remaining variance.

The decline in microbial diversity, as indicated by the Shannon Index, mirrors trends observed in other chronic and inflammatory diseases, suggesting that changes in the microbiome may influence disease progression or reflect immune system deterioration.

Overall, these findings indicate that disruptions in microbial composition across the disease continuum offer important insights into the initial phases of dysregulation and possible pathways that could lead to more severe disease outcomes. Such bacterial imbalances may result in alterations of microbiota-derived metabolites, which serve as signaling molecules and substrates

for immune and metabolic responses, potentially influencing the progression of MM. Furthermore, these findings could help identify predictive biomarkers for the transition from MGUS to MM.

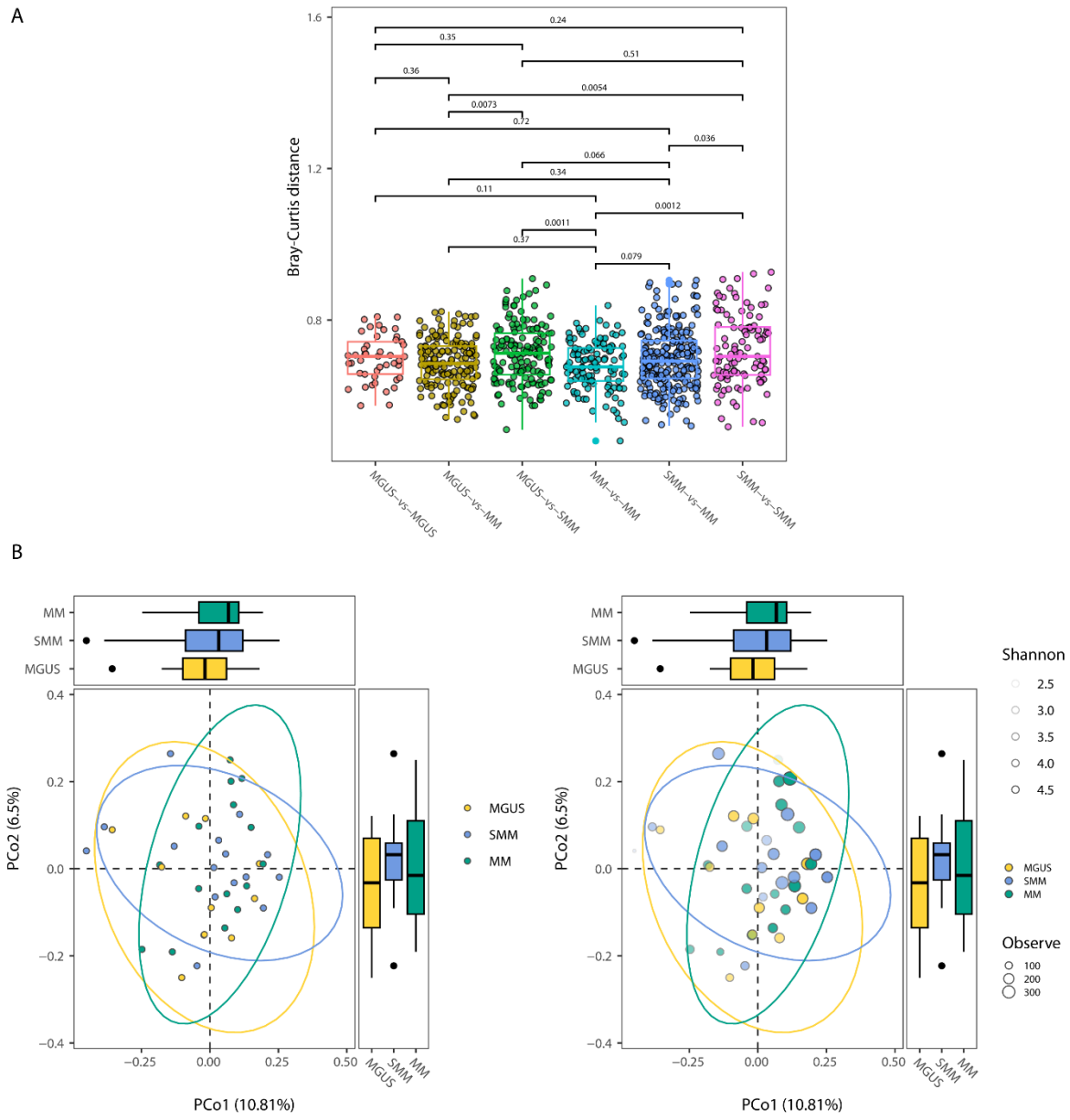

Figure 12. Bray-Curtis distance, principal coordinates analysis (PCoA) and Shannon diversity index of microbial communities across MGUS, SMM, and MM stages

(A) Box-plots displaying the Bray-Curtis distance, representing the dissimilarity in microbiome composition between different patient groups. Each group comparison is shown along the x-axis, while the y-axis represents the calculated Bray-Curtis distance. The comparisons between groups include: “MGUS vs MGUS”, “SMM vs SMM”, and “MM vs MM” as control. (B) Figure showing the PCoA plot of microbial community composition across different disease stages. The PCoA plot displays the first two principal coordinates (PCo1: 10.81% of variance, PCo2: 6.5% of variance), which together explain 17.31% of the overall variation between samples. Distinct clustering indicates compositional differences between disease stages. The Shannon diversity index, represented by color gradients, measures the microbial diversity within each sample, with higher values (lighter colors) indicating greater species richness and evenness, typically associated with early disease stages (MGUS), while lower values (darker colors) indicate reduced diversity, often linked to advanced disease (MM).

Part V

Over the recent years, significant improvement has been made in managing MM, allowing patients to experience better outcomes and quality of life. Among the various therapeutic and monitoring strategies, minimal residual disease (MRD) analysis has emerged as a crucial tool for assessing treatment response and outcomes (146,147). Specifically, MRD refers to the disease burden that remains following therapeutic intervention and may be detectable by highly sensitive assays (148). Currently, MRD is the most powerful predictor of progression and survival in MM (149,150). The detection and quantification of MRD offer valuable insights into treatment efficacy, relapse risk, and the necessity for additional interventions. Importantly, MRD results should be interpreted alongside other clinical and biological factors that may affect the prognosis and treatment response of MM patients.

The IMWG MRD criteria state that MRD should be assessed when a patient achieves complete response or better, with a minimum sensitivity of 1 nucleated tumor cell in 100.000 normal cells (10^−5 sensitivity threshold), by either next-generation sequencing (NGS) or next-generation flow cytometry (NGF) (146).

NGF employs fluorescent antibodies to detect myeloma cells by analyzing their immunophenotypic characteristics, along with innovative software that aggregates results to enhance sensitivity. In contrast, NGS relies on molecular markers unique to each patient's myeloma clone, such as immunoglobulin gene rearrangements and somatic mutations (146,147). Detecting MRD through NGF provides the additional benefit of delivering comprehensive insights into the overall bone marrow composition. This method allows for precise identification and characterization of key immune populations at single-cell resolution, creating an intricate map of immune population distribution that correlates with clinical outcomes.

In this section of the project, differences in the composition of the BM immune microenvironment were analyzed at baseline and during MRD assessment. This analysis supports the hypothesis that the immune microenvironment is crucial in determining the depth and duration of treatment response. The analysis was conducted using BM aspirates from 20 MM patients, collected at diagnosis and post-treatment, and performed using NGF and FlowCT (115). This study compared patients who achieved sustained MRD negativity (n=11) with those who either never achieved or were unable to maintain MRD negativity (n=9). Thirteen patients were treated with Dara-VTD (Daratumumab combined with Bortezomib, Thalidomide, and Dexamethasone), one patient received Dara-VD (Daratumumab combined with Bortezomib and Dexamethasone), three patients were treated with Dara-RD (Daratumumab combined with Lenalidomide and Dexamethasone),

two patients received VTD (Bortezomib, Thalidomide, and Dexamethasone), and one patient was treated with VCD (Bortezomib, Cyclophosphamide, and Dexamethasone) (**Table 2**).

Table 2. Clinical characteristics of MM patients

Characteristic	MRD negative	MRD positive
Number of patients	n= 12 (60%)[1]	n= 8 (40%)[1]
Therapy		
Dara + RD	1 (8.3%)	2 (25%)
Dara + VD	0 (0%)	1 (13%)
Dara + VTD	9 (75%)	4 (50%)
VCD	1 (8.3%)	0 (0%)
VTD	1 (8.3%)	1 (13%)

[1]n (%)

The analysis of the PCD tube revealed a significant decrease at follow-up in the frequency of granulocytes (p=0.0012), plasma cells (p=0.029), and T lymphocytes (p=0.011), particularly naïve $CD81^+$ T cells (p=2.9e-05), as well as in the $CD28^-CD27^-CD81^+CD117^-$ T/NK population. At the same time, there was a significant rise in erythroblasts (p=0.000043) and B lymphocytes (p=0.0013), especially in $CD38^+$ B cells (p=0.03) (**Figure 13C**). When comparing patients with persistent MRD to those with undetectable MRD, the latter group showed a higher baseline granulocyte-to-lymphocyte ratio (p=0.038) (**Figure 13D)**. Further follow-up assessments found an increase in both erythroblasts and B lymphocytes in the undetectable MRD group (p=0.031 and p=0.045, respectively) (**Figure 13E).**

In the PCST tube, similar trends to those in the PCD tube were observed, along with an increase in the NK $CD56^+/CD56^{dim}$ ratio (p=0.035) and a decrease in the $CD56^{dim}$ NK population (p=0.0091) from baseline to follow-up (**Figure 14C**). Additionally, patients with undetectable MRD had a lower percentage of NK CD56dim cells compared to those with persistent MRD at follow-up (p=0.014) (**Figure 14E**).

The detailed analysis of BM immune populations provides valuable insights into the complex immunological landscape associated with MRD status in MM. Emerging evidence suggests that distinct immune signatures not only correlate with MRD status but may also serve as reliable biomarkers for predicting patient response to therapy. These findings highlight the potential to refine risk stratification and tailor treatment approaches based on individual immune profiles, ultimately paving the way for more personalized and targeted therapeutic strategies in MM.

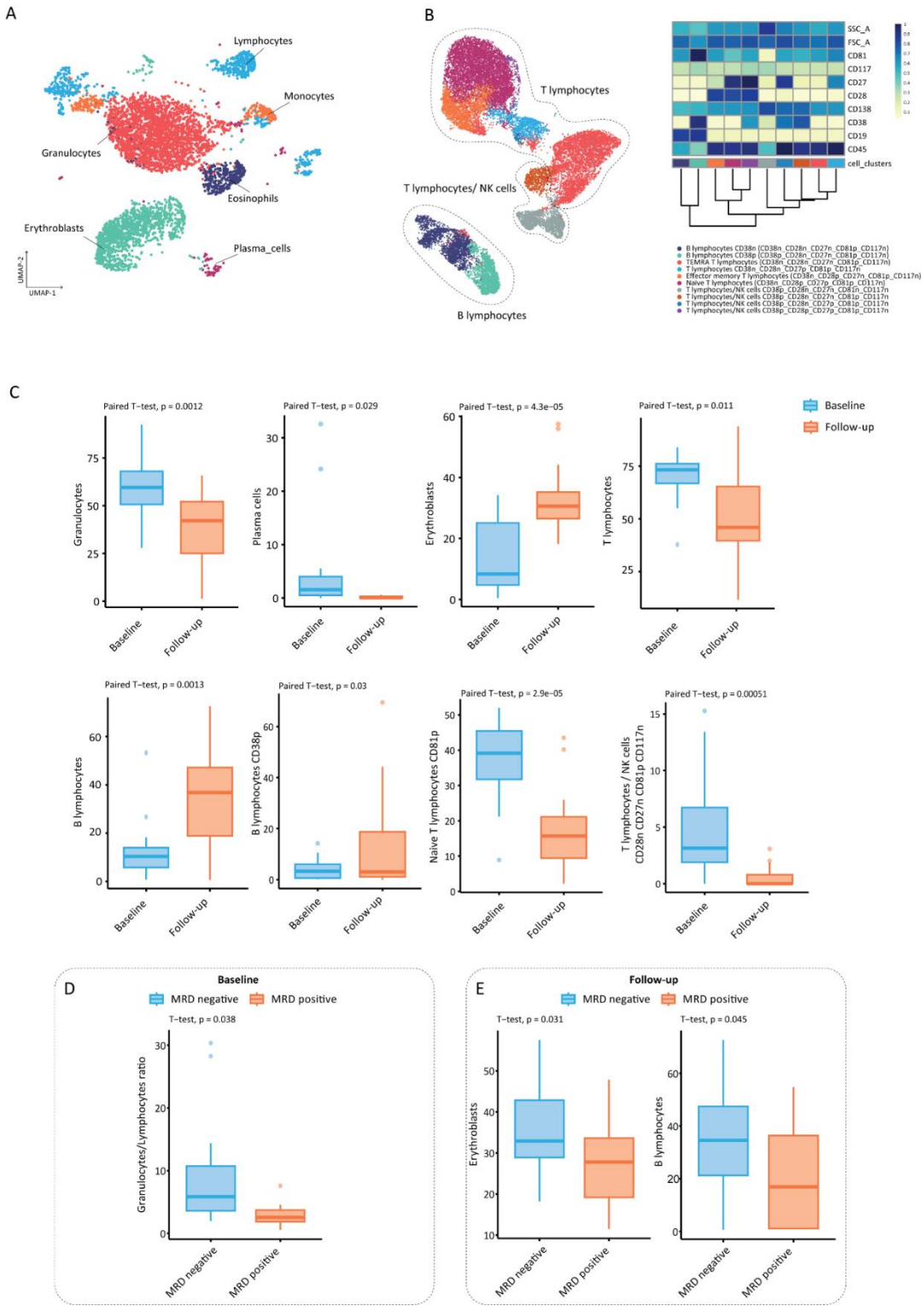

Figure 13. Immune profiling of MRD-positive and MRD-negative MM patients using the PCD tube
(A) Uniform manifold approximation and projection (UMAP) of eosinophils ($CD45^{+bright}$, SCC^{high}), erythroblasts ($CD45^{-}$, $CD38^{-}$, SCC^{low}), granulocytes ($CD45^{+dim}$, SCC^{high}), lymphocytes ($CD45^{+}$, SCC^{low}), monocytes ($CD45^{+}$, SCC^{int}) and plasma cells ($CD138^{+}$ $CD38^{+high}$) identified by self-organizing map (SOM) of BD OneFlow™ PCD tube. (B) Lymphocyte subsets were subclustered based on the median expression of individual markers within each cell cluster, accompanied by a heatmap illustrating the mean expression of each marker across all identified clusters. (C) Box plots showing the differential distribution of immune cell subsets at baseline and follow-up. (D) Box plot depicting the ratio of granulocyte to lymphocyte frequencies at baseline between MRD-positive and MRD-negative MM patients. (E) Box plot representing the frequency of erythroblasts and B lymphocytes at follow-up between MRD-positive and MRD-negative MM patients.

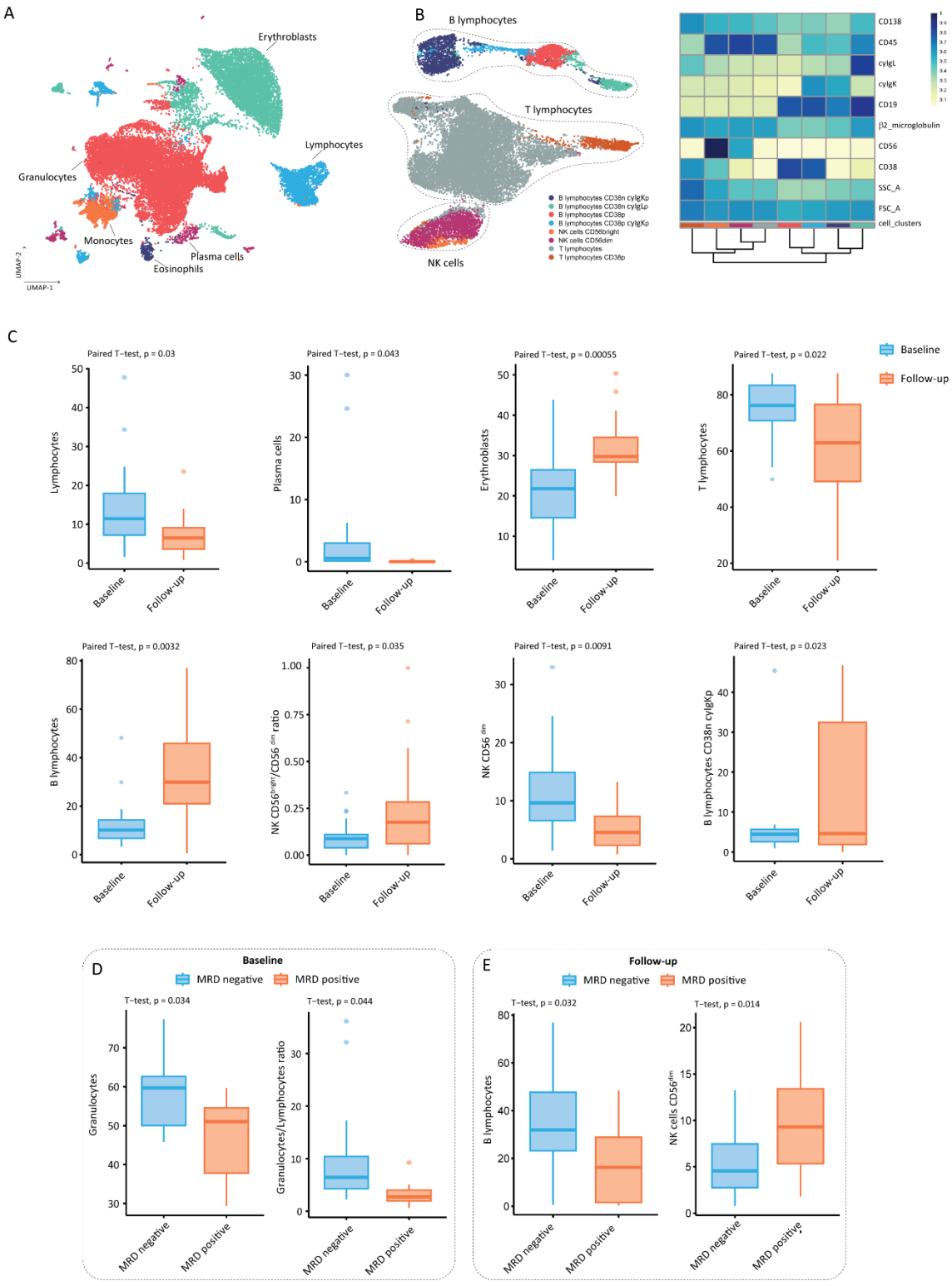

Figure 14. Immune profiling of MRD-positive and MRD-negative MM patients using the PCD tube

(A) Uniform manifold approximation and projection (UMAP) of eosinophils ($CD45^{+bright}$, SCC^{high}), erythroblasts ($CD45^{-}$, $CD38^{-}$, SCC^{low}), granulocytes ($CD45^{+dim}$, SCC^{high}), lymphocytes ($CD45^{+}$, SCC^{low}), monocytes ($CD45^{+}$, SCC^{int}) and plasma cells ($CD138^{+}$ $CD38^{+high}$) identified by self-organizing map (SOM) of BD OneFlow™ PCST tube. (B) Lymphocyte subsets were subclustered based on the median expression of individual markers within each cell cluster, accompanied by a heatmap illustrating the mean expression of each marker across all identified clusters. (C) Box plots showing the differential distribution of immune cell subsets at baseline and follow-up. (D) Box plot depicting the ratio of granulocyte to lymphocyte frequencies at baseline between MRD-positive and MRD-negative MM patients. (E) Box plot representing the frequency of erythroblasts and B lymphocytes at follow-up between MRD-positive and MRD-negative MM patients.

Discussion

The findings presented in this thesis highlight the pivotal role of the immune microenvironment in the progression of monoclonal gammopathies (MGUS, SMM, and MM) and provide valuable insights into therapeutic strategies to improve patient outcomes in MM. By focusing on the immune system's interactions with malignant cells and the BM microenvironment, the research identifies key factors that drive disease progression and response to therapy, while offering new avenues for intervention.

The analysis of ferritin metabolism revealed its dual role in MM progression, where it not only reflects disturbances in iron homeostasis but also plays a direct role in supporting malignant plasma cell growth.

Moreover, the immune microenvironment undergoes significant alterations as MGUS progresses to active MM. Using advanced techniques like FlowCT, these changes were mapped, particularly the shifts in granulocyte and lymphocyte populations. A decline in granulocytes, alongside a rise in T lymphocytes, was observed as the disease advanced. Significantly, a higher granulocyte-to-lymphocyte ratio (GLR) and granulocyte-to-T lymphocyte ratio (GTL) were associated with improved outcomes, especially in patients treated with Daratumumab, suggesting that these ratios could serve as predictive markers for therapy response. The BM's role in enhancing Daratumumab's efficacy, mainly through granulocyte-mediated cytotoxicity, highlights the importance of the tumor microenvironment in shaping treatment success. Moreover, γδ T cells were found to lose functionality as MM developed progressively. Markers of immune exhaustion, such as TIM3 and PD1, were significantly upregulated in these cells, indicating their impaired ability to control tumor growth. This study emphasizes the potential of targeting these exhaustion pathways to reinvigorate the immune response against MM. The correlation between TIM3 expression and patient outcomes further suggests that immune exhaustion markers could serve as therapeutic targets and indicators of disease progression.

The study also explored the complex interactions with cytokines, chemokines, and microbiota communities. The decline in various immune mediators reflected the weakening of the immune system's capacity to mount an effective response against the tumor. Moreover, the gut microbiota composition was altered in patients with MM, with an increased prevalence of pro-inflammatory bacterial species. This suggests that systemic inflammation and local microbiota imbalances may contribute to disease progression.

Additionally, MRD analysis proved crucial in assessing treatment response and predicting long-term outcomes. Differences in the immune microenvironment between MRD-negative and MRD-positive patients revealed that specific immune populations are involved in eliminating residual disease. By integrating immune profiling with MRD assessments, these results pave the way for

more personalized approaches in monitoring patient response and identifying those at risk of relapse.

In conclusion, by identifying immune exhaustion markers, modulating iron metabolism, and leveraging immune cell subsets as predictive indicators, this research paves the way for therapies designed to enhance anti-tumor immunity. This project deepens our understanding of the immune microenvironment's role in monoclonal gammopathies, uncovering novel biomarkers to help stratify patients and pinpoint those most likely to benefit from specific therapies. These insights could drive the development of more personalized and effective treatment approaches, offering new hope for improved management of MM and enhanced patient survival.

References

1. Siegel RL, Giaquinto AN, Jemal A. Cancer statistics, 2024. CA Cancer J Clin. 2024 Jan;74(1):12–49.

2. Rajkumar SV, Dimopoulos MA, Palumbo A, Blade J, Merlini G, Mateos MV, et al. International Myeloma Working Group updated criteria for the diagnosis of multiple myeloma. Lancet Oncol. 2014 Nov;15(12):e538–48.

3. Zuern K, Hielscher T, Werly A, Breitkreutz I, Sauer S, Raab MS, et al. Longitudinal assessment of established risk stratification models in patients with monoclonal gammopathy of undetermined significance. Blood Cancer J. 2024 Aug 27;14(1):148.

4. Rajkumar SV, Kyle RA, Therneau TM, Melton LJ, Bradwell AR, Clark RJ, et al. Serum free light chain ratio is an independent risk factor for progression in monoclonal gammopathy of undetermined significance. Blood. 2005 Aug 1;106(3):812–7.

5. Turesson I, Kovalchik SA, Pfeiffer RM, Kristinsson SY, Goldin LR, Drayson MT, et al. Monoclonal gammopathy of undetermined significance and risk of lymphoid and myeloid malignancies: 728 cases followed up to 30 years in Sweden. Blood. 2014 Jan 16;123(3):338–45.

6. Pérez-Persona E, Vidriales MB, Mateo G, García-Sanz R, Mateos MV, De Coca AG, et al. New criteria to identify risk of progression in monoclonal gammopathy of uncertain significance and smoldering multiple myeloma based on multiparameter flow cytometry analysis of bone marrow plasma cells. Blood. 2007 Oct 1;110(7):2586–92.

7. Pérez-Persona E, Mateo G, García-Sanz R, Mateos M, De Las Heras N, De Coca AG, et al. Risk of progression in smouldering myeloma and monoclonal gammopathies of unknown significance: comparative analysis of the evolution of monoclonal component and multiparameter flow cytometry of bone marrow plasma cells. Br J Haematol. 2010 Jan;148(1):110–4.

8. Pérez-Escurza O, Flores-Montero J, Óskarsson JÞ, Sanoja-Flores L, Del Pozo J, Lecrevisse Q, et al. Immunophenotypic assessment of clonal plasma cells and B-cells in bone marrow and blood in the diagnostic classification of early stage monoclonal gammopathies: an iSTOPMM study. Blood Cancer J. 2023 Dec 11;13(1):182.

9. Mouhieddine TH. How to Identify and Manage High-Risk Smoldering Multiple Myeloma. Curr Oncol Rep [Internet]. 2024 Aug 23 [cited 2024 Oct 2]; Available from: https://link.springer.com/10.1007/s11912-024-01596-5

10. Mateos MV, Kumar S, Dimopoulos MA, González-Calle V, Kastritis E, Hajek R, et al. International Myeloma Working Group risk stratification model for smoldering multiple myeloma (SMM). Blood Cancer J. 2020 Oct 16;10(10):102.

11. Dispenzieri A, Kyle RA, Katzmann JA, Therneau TM, Larson D, Benson J, et al. Immunoglobulin free light chain ratio is an independent risk factor for progression of smoldering (asymptomatic) multiple myeloma. Blood. 2008 Jan 15;111(2):785–9.

12. Lakshman A, Rajkumar SV, Buadi FK, Binder M, Gertz MA, Lacy MQ, et al. Risk stratification of smoldering multiple myeloma incorporating revised IMWG diagnostic criteria. Blood Cancer J. 2018 Jun 12;8(6):59.

13. Ravi P, Kumar S, Larsen JT, Gonsalves W, Buadi F, Lacy MQ, et al. Evolving changes in disease biomarkers and risk of early progression in smoldering multiple myeloma. Blood Cancer J. 2016 Jul 29;6(7):e454–e454.

14. Fernández De Larrea C, Isola I, Pereira A, Cibeira MT, Magnano L, Tovar N, et al. Evolving M-protein pattern in patients with smoldering multiple myeloma: impact on early progression. Leukemia. 2018 Jun;32(6):1427–34.

15. Wu V, Moshier E, Leng S, Barlogie B, Cho HJ, Jagannath S, et al. Risk stratification of smoldering multiple myeloma: predictive value of free light chains and group-based trajectory modeling. Blood Adv. 2018 Jun 26;2(12):1470–9.

16. De Daniel A, Rodríguez-Lobato LG, Tovar N, Cibeira MT, Moreno DF, Oliver-Caldés A, et al. The evolving pattern of the monoclonal protein improves the IMWG 2/20/20 classification for patients with smoldering multiple myeloma. HemaSphere. 2024 May;8(5):e76.

17. Bustoros M, Sklavenitis-Pistofidis R, Park J, Redd R, Zhitomirsky B, Dunford AJ, et al. Genomic Profiling of Smoldering Multiple Myeloma Identifies Patients at a High Risk of Disease Progression. J Clin Oncol. 2020 Jul 20;38(21):2380–9.

18. Termini R, Žihala D, Terpos E, Perez-Montaña A, Jelínek T, Raab M, et al. Circulating Tumor and Immune Cells for Minimally Invasive Risk Stratification of Smoldering Multiple Myeloma. Clin Cancer Res. 2022 Nov 1;28(21):4771–81.

19. Cowan A, Ferrari F, Freeman SS, Redd R, El-Khoury H, Perry J, et al. Personalised progression prediction in patients with monoclonal gammopathy of undetermined significance or smouldering multiple myeloma (PANGEA): a retrospective, multicohort study. Lancet Haematol. 2023 Mar;10(3):e203–12.

20. Mateos MV, Martínez-López J, Rodriguez Otero P, González-Calle V, Gonzalez MS, Oriol A, et al. Curative Strategy for High-Risk Smoldering Myeloma: Carfilzomib, Lenalidomide, and Dexamethasone (KRd) Followed by Transplant, KRd Consolidation, and Rd Maintenance. J Clin Oncol. 2024 Sep 20;42(27):3247–56.

21. Paiva B, Mateos MV, Sanchez-Abarca LI, Puig N, Vidriales MB, López-Corral L, et al. Immune status of high-risk smoldering multiple myeloma patients and its therapeutic modulation under LenDex: a longitudinal analysis. Blood. 2016 Mar 3;127(9):1151–62.

22. Mateos MV, Hernández MT, Giraldo P, De La Rubia J, De Arriba F, Corral LL, et al. Lenalidomide plus dexamethasone versus observation in patients with high-risk smouldering multiple myeloma (QuiRedex): long-term follow-up of a randomised, controlled, phase 3 trial. Lancet Oncol. 2016 Aug;17(8):1127–36.

23. Lonial S, Jacobus S, Fonseca R, Weiss M, Kumar S, Orlowski RZ, et al. Randomized Trial of Lenalidomide Versus Observation in Smoldering Multiple Myeloma. J Clin Oncol. 2020 Apr 10;38(11):1126–37.

24. Dimopoulos MA, Voorhees PM, Goldschmidt H, Baker RI, Shi Y, Rousseau E, et al. Subcutaneous daratumumab (DARA SC) versus active monitoring in patients (pts) with high-risk smoldering multiple myeloma (SMM): Randomized, open-label, phase 3 AQUILA study. J Clin Oncol. 2022 Jun 1;40(16_suppl):TPS8075–TPS8075.

25. Nadeem O, Redd R, Mo CC, Laubach J, Prescott J, Metivier A, et al. B-PRISM (Precision Intervention Smoldering Myeloma): A phase II trial of combination of daratumumab, bortezomib,

lenalidomide, and dexamethasone in high-risk smoldering multiple myeloma. J Clin Oncol. 2022 Jun 1;40(16_suppl):8040–8040.

26. Kumar SK, Alsina M, Laplant B, Badros AZ, Abdallah AO, Abonour R, et al. Fixed Duration Therapy with Daratumumab, Carfilzomib, Lenalidomide and Dexamethasone for High Risk Smoldering Multiple Myeloma-Results of the Ascent Trial. Blood. 2022 Nov 15;140(Supplement 1):1830–2.

27. Manasanch EE, Jagannath S, Lee HC, Patel KK, Graham C, Kaufman GP, et al. A Multicenter Phase II Single Arm Trial of Isatuximab in Patients with High Risk Smoldering Multiple Myeloma (HRSMM). Blood. 2019 Nov 13;134(Supplement_1):3116–3116.

28. Mateos MV, Rodriguez Otero P, Koh Y, Martinez-Lopez J, Parmar G, Prince HM, et al. Isatuximab in Combination with Lenalidomide and Dexamethasone in Patients with High-Risk Smoldering Multiple Myeloma: Updated Safety Run-in Results from the Randomized Phase 3 Ithaca Study. Blood. 2022 Nov 15;140(Supplement 1):7317–9.

29. Jagannath S, Laubach J, Wong E, Stockerl-Goldstein K, Rosenbaum C, Dhodapkar M, et al. Elotuzumab monotherapy in patients with smouldering multiple myeloma: a phase 2 study. Br J Haematol. 2018 Aug;182(4):495–503.

30. Manasanch EE, Han G, Mathur R, Qing Y, Zhang Z, Lee H, et al. A pilot study of pembrolizumab in smoldering myeloma: report of the clinical, immune, and genomic analysis. Blood Adv. 2019 Aug 13;3(15):2400–8.

31. Brighton TA, Khot A, Harrison SJ, Ghez D, Weiss BM, Kirsch A, et al. Randomized, Double-Blind, Placebo-Controlled, Multicenter Study of Siltuximab in High-Risk Smoldering Multiple Myeloma. Clin Cancer Res. 2019 Jul 1;25(13):3772–5.

32. Ferla V, Farina F, Perini T, Marcatti M, Ciceri F. Monoclonal Antibodies in Smoldering Multiple Myeloma and Monoclonal Gammopathy of Undetermined Significance: Current Status and Future Directions. Pharmaceuticals. 2024 Jul 6;17(7):901.

33. Nadeem O, Redd R, Stampleman LV, Matous JV, Yee AJ, Zonder JA, et al. A Phase II Study of Daratumumab in Patients with High-Risk MGUS and Low-Risk Smoldering Multiple Myeloma: First Report of Efficacy and Safety. Blood. 2019 Nov 13;134(Supplement_1):1898–1898.

34. Pawlyn C, Morgan GJ. Evolutionary biology of high-risk multiple myeloma. Nat Rev Cancer. 2017 Sep;17(9):543–56.

35. Caprio C, Sacco A, Giustini V, Roccaro AM. Epigenetic Aberrations in Multiple Myeloma. Cancers. 2020 Oct 15;12(10):2996.

36. Clarke SE, Fuller KA, Erber WN. Chromosomal defects in multiple myeloma. Blood Rev. 2024 Mar;64:101168.

37. Plano F, Corsale AM, Gigliotta E, Camarda G, Vullo C, Di Simone M, et al. Monoclonal Gammopathies and the Bone Marrow Microenvironment: From Bench to Bedside and Then Back Again. Hematol Rep. 2023 Jan 9;15(1):23–49.

38. Yi Z, Ma T, Liu J, Tie W, Li Y, Bai J, et al. The yin–yang effects of immunity: From monoclonal gammopathy of undetermined significance to multiple myeloma. Front Immunol. 2022 Jul 25;13:925266.

39. Sklavenitis-Pistofidis R, Aranha MP, Redd RA, Baginska J, Haradhvala NJ, Hallisey M, et al. Immune biomarkers of response to immunotherapy in patients with high-risk smoldering myeloma. Cancer Cell. 2022 Nov;40(11):1358-1373.e8.

40. Larrayoz M, Garcia-Barchino MJ, Celay J, Etxebeste A, Jimenez M, Perez C, et al. Preclinical models for prediction of immunotherapy outcomes and immune evasion mechanisms in genetically heterogeneous multiple myeloma. Nat Med. 2023 Mar;29(3):632–45.

41. Friedrich MJ, Neri P, Kehl N, Michel J, Steiger S, Kilian M, et al. The pre-existing T cell landscape determines the response to bispecific T cell engagers in multiple myeloma patients. Cancer Cell. 2023 Apr;41(4):711-725.e6.

42. Wang J, Zheng Y, Tu C, Zhang H, Vanderkerken K, Menu E, et al. Identification of the immune checkpoint signature of multiple myeloma using mass cytometry-based single-cell analysis. Clin Transl Immunol. 2020 Jan;9(5):e1132.

43. Zavidij O, Haradhvala NJ, Mouhieddine TH, Sklavenitis-Pistofidis R, Cai S, Reidy M, et al. Single-cell RNA sequencing reveals compromised immune microenvironment in precursor stages of multiple myeloma. Nat Cancer. 2020 Apr 27;1(5):493–506.

44. Robinson MH, Villa NY, Jaye DL, Nooka AK, Duffy A, McCachren SS, et al. Regulation of antigen-specific T cell infiltration and spatial architecture in multiple myeloma and premalignancy. J Clin Invest. 2023 Aug 1;133(15):e167629.

45. Bailur JK, McCachren SS, Doxie DB, Shrestha M, Pendleton K, Nooka AK, et al. Early alterations in stem-like/marrow-resident T cells and innate and myeloid cells in preneoplastic gammopathy. JCI Insight. 2019 Jun 6;4(11):e127807.

46. Koike M, Sekigawa I, Okada M, Matsumoto M, Iida N, Hashimoto H, et al. Relationship between CD4+/CD8+ T cell ratio and T cell activation in multiple myeloma: reference to IL-16. Leuk Res. 2002 Aug;26(8):705–11.

47. Pessoa De Magalhaes RJ, Vidriales MB, Paiva B, Fernandez-Gimenez C, Garcia-Sanz R, Mateos MV, et al. Analysis of the immune system of multiple myeloma patients achieving long-term disease control by multidimensional flow cytometry. Haematologica. 2013 Jan 1;98(1):79–86.

48. Feng P, Yan R, Dai X, Xie X, Wen H, Yang S. The Alteration and Clinical Significance of Th1/Th2/Th17/Treg Cells in Patients with Multiple Myeloma. Inflammation. 2015 Apr;38(2):705–9.

49. Ogawara H, Handa H, Yamazaki T, Toda T, Yoshida K, Nishimoto N, et al. High Th1/Th2 ratio in patients with multiple myeloma. Leuk Res. 2005 Feb;29(2):135–40.

50. Botta C, Perez C, Larrayoz M, Puig N, Cedena MT, Termini R, et al. Large T cell clones expressing immune checkpoints increase during multiple myeloma evolution and predict treatment resistance. Nat Commun. 2023 Sep 20;14(1):5825.

51. Schinke C, Poos AM, Bauer M, John L, Johnson S, Deshpande S, et al. Characterizing the role of the immune microenvironment in multiple myeloma progression at a single-cell level. Blood Adv. 2022 Nov 22;6(22):5873–83.

52. Racanelli V, Leone P, Frassanito MA, Brunetti C, Perosa F, Ferrone S, et al. Alterations in the antigen processing-presenting machinery of transformed plasma cells are associated with reduced recognition by CD8+ T cells and characterize the progression of MGUS to multiple myeloma. Blood. 2010 Feb 11;115(6):1185–93.

53. Zelle-Rieser C, Thangavadivel S, Biedermann R, Brunner A, Stoitzner P, Willenbacher E, et al. T cells in multiple myeloma display features of exhaustion and senescence at the tumor site. J Hematol OncolJ Hematol Oncol. 2016 Dec;9(1):116.

54. Guillerey C, Harjunpää H, Carrié N, Kassem S, Teo T, Miles K, et al. TIGIT immune checkpoint blockade restores CD8+ T-cell immunity against multiple myeloma. Blood. 2018 Oct 18;132(16):1689–94.

55. Minnie SA, Kuns RD, Gartlan KH, Zhang P, Wilkinson AN, Samson L, et al. Myeloma escape after stem cell transplantation is a consequence of T-cell exhaustion and is prevented by TIGIT blockade. Blood. 2018 Oct 18;132(16):1675–88.

56. Kulikowska De Nałęcz A, Ciszak L, Usnarska-Zubkiewicz L, Pawlak E, Frydecka I, Szmyrka M, et al. Inappropriate Expression of PD-1 and CTLA-4 Checkpoints in Myeloma Patients Is More Pronounced at Diagnosis: Implications for Time to Progression and Response to Therapeutic Checkpoint Inhibitors. Int J Mol Sci. 2023 Mar 17;24(6):5730.

57. Pilcher WC, Yao L, Gonzalez-Kozlova E, Pita-Juarez Y, Karagkouni D, Acharya CR, et al. A single-cell atlas characterizes dysregulation of the bone marrow immune microenvironment associated with outcomes in multiple myeloma [Internet]. 2024 [cited 2024 Oct 14]. Available from: http://biorxiv.org/lookup/doi/10.1101/2024.05.15.593193

58. John L, Poos AM, Brobeil A, Schinke C, Huhn S, Prokoph N, et al. Resolving the spatial architecture of myeloma and its microenvironment at the single-cell level. Nat Commun. 2023 Aug 17;14(1):5011.

59. Bryant C, Suen H, Brown R, Yang S, Favaloro J, Aklilu E, et al. Long-term survival in multiple myeloma is associated with a distinct immunological profile, which includes proliferative cytotoxic T-cell clones and a favourable Treg/Th17 balance. Blood Cancer J. 2013 Sep 13;3(9):e148–e148.

60. Lad D, Huang Q, Hoeppli R, Garcia R, Xu L, Levings M, et al. Evaluating the role of Tregs in the progression of multiple myeloma. Leuk Lymphoma. 2019 Jul 29;60(9):2134–42.

61. Prabhala RH, Pelluru D, Fulciniti M, Prabhala HK, Nanjappa P, Song W, et al. Elevated IL-17 produced by Th17 cells promotes myeloma cell growth and inhibits immune function in multiple myeloma. Blood. 2010 Jul 1;115(26):5385–92.

62. Shen CJ, Yuan ZH, Liu YX, Hu GY. Increased Numbers of T Helper 17 Cells and the Correlation with Clinicopathological Characteristics in Multiple Myeloma. J Int Med Res. 2012 Apr;40(2):556–64.

63. Ma T, Zhang Y, Zhou X, Xie P, Li J. A Unique Role of T Helper 17 Cells in Different Treatment Stages of Multiple Myeloma. Clin Lymphoma Myeloma Leuk. 2020 Mar;20(3):190–7.

64. Dhodapkar KM, Barbuto S, Matthews P, Kukreja A, Mazumder A, Vesole D, et al. Dendritic cells mediate the induction of polyfunctional human IL17-producing cells (Th17-1 cells) enriched in the bone marrow of patients with myeloma. Blood. 2008 Oct 1;112(7):2878–85.

65. Hadjiaggelidou C, Katodritou E. Regulatory T-Cells and Multiple Myeloma: Implications in Tumor Immune Biology and Treatment. J Clin Med. 2021 Oct 5;10(19):4588.

66. Chen H, Wang X, Wang Y, Chang X. What happens to regulatory T cells in multiple myeloma. Cell Death Discov. 2023 Dec 21;9(1):468.

67. Giannopoulos K, Kaminska W, Hus I, Dmoszynska A. The frequency of T regulatory cells modulates the survival of multiple myeloma patients: detailed characterisation of immune status in multiple myeloma. Br J Cancer. 2012 Jan;106(3):546–52.

68. Ma Y, Lei H, Tan J, Xuan L, Wu X, Liu Q. Characterization of γδ regulatory T cells from peripheral blood in patients with multiple myeloma. Biochem Biophys Res Commun. 2016 Nov;480(4):594–601.

69. Alrasheed N, Lee L, Ghorani E, Henry JY, Conde L, Chin M, et al. Marrow-Infiltrating Regulatory T Cells Correlate with the Presence of Dysfunctional CD4+PD-1+ Cells and Inferior Survival in Patients with Newly Diagnosed Multiple Myeloma. Clin Cancer Res. 2020 Jul 1;26(13):3443–54.

70. Muthu Raja KR, Rihova L, Zahradova L, Klincova M, Penka M, Hajek R. Increased T Regulatory Cells Are Associated with Adverse Clinical Features and Predict Progression in Multiple Myeloma. Rieux-Laucat F, editor. PLoS ONE. 2012 Oct 10;7(10):e47077.

71. Aref S, Azmy E, El-Gilany AH. Upregulation of CD200 is associated with regulatory T cell expansion and disease progression in multiple myeloma. Hematol Oncol. 2017 Mar;35(1):51–7.

72. Marsh-Wakefield F, Kruzins A, McGuire HM, Yang S, Bryant C, Fazekas De St. Groth B, et al. Mass Cytometry Discovers Two Discrete Subsets of CD39−Treg Which Discriminate MGUS From Multiple Myeloma. Front Immunol. 2019 Aug 2;10:1596.

73. Prabhala RH, Neri P, Bae JE, Tassone P, Shammas MA, Allam CK, et al. Dysfunctional T regulatory cells in multiple myeloma. Blood. 2006 Jan 1;107(1):301–4.

74. Foglietta M, Castella B, Mariani S, Coscia M, Godio L, Ferracini R, et al. The bone marrow of myeloma patients is steadily inhabited by a normal-sized pool of functional regulatory T cells irrespectiveof the disease status. Haematologica. 2014 Oct 1;99(10):1605–10.

75. Braga WMT, Da Silva BR, De Carvalho AC, Maekawa YH, Bortoluzzo AB, Rizzatti EG, et al. FOXP3 and CTLA4 overexpression in multiple myeloma bone marrow as a sign of accumulation of CD4+ T regulatory cells. Cancer Immunol Immunother. 2014 Nov;63(11):1189–97.

76. Gupta R, Ganeshan P, Hakim M, Verma R, Sharma A, Kumar L. Significantly reduced regulatory T cell population in patients with untreated multiple myeloma. Leuk Res. 2011 Jul;35(7):874–8.

77. D'Arena G, Rossi G, Laurenti L, Statuto T, D'Auria F, Valvano L, et al. Circulating Regulatory T-Cells in Monoclonal Gammopathies of Uncertain Significance and Multiple Myeloma: In Search of a Role. J Immunol Res. 2016;2016:1–7.

78. Feyler S, Von Lilienfeld-Toal M, Jarmin S, Marles L, Rawstron A, Ashcroft AJ, et al. $CD4^+$ $CD25^+$ $FoxP3^+$ regulatory T cells are increased whilst $CD3^+$ $CD4^-$ $CD8^-$ $\alpha\beta TCR^+$ Double Negative T cells are decreased in the peripheral blood of patients with multiple myeloma which correlates with disease burden. Br J Haematol. 2009 Mar;144(5):686–95.

79. Beyer M, Kochanek M, Giese T, Endl E, Weihrauch MR, Knolle PA, et al. In vivo peripheral expansion of naive CD4+CD25highFoxP3+ regulatory T cells in patients with multiple myeloma. Blood. 2006 May 15;107(10):3940–9.

80. Wang J nuo, Cao X xin, Zhao A lin, Cai H, Wang X, Li J. Increased activated regulatory T cell subsets and aging Treg-like cells in multiple myeloma and monoclonal gammopathy of undetermined significance: a case control study. Cancer Cell Int. 2018 Dec;18(1):187.

81. Papadimitriou K, Tsakirakis N, Malandrakis P, Vitsos P, Metousis A, Orologas-Stavrou N, et al. Deep Phenotyping Reveals Distinct Immune Signatures Correlating with Prognostication, Treatment Responses, and MRD Status in Multiple Myeloma. Cancers. 2020 Nov 4;12(11):3245.

82. Szudy-Szczyrek A, Ahern S, Kozioł M, Majowicz D, Szczyrek M, Krawczyk J, et al. Therapeutic Potential of Innate Lymphoid Cells for Multiple Myeloma Therapy. Cancers. 2021 Sep 26;13(19):4806.

83. Zhang L, Peng X, Ma T, Liu J, Yi Z, Bai J, et al. Natural killer cells affect the natural course, drug resistance, and prognosis of multiple myeloma. Front Cell Dev Biol. 2024 Feb 12;12:1359084.

84. Venglar O, Bago JR, Motais B, Hajek R, Jelinek T. Natural Killer Cells in the Malignant Niche of Multiple Myeloma. Front Immunol. 2022 Jan 11;12:816499.

85. D'Souza C, Keam SP, Yeang HXA, Neeson M, Richardson K, Hsu AK, et al. Myeloma natural killer cells are exhausted and have impaired regulation of activation. Haematologica. 2021 May 20;106(9):2522–6.

86. Sun J, Park C, Guenthner N, Gurley S, Zhang L, Lubben B, et al. Tumor-associated macrophages in multiple myeloma: advances in biology and therapy. J Immunother Cancer. 2022 Apr;10(4):e003975.

87. Cencini E, Sicuranza A, Ciofini S, Fabbri A, Bocchia M, Gozzetti A. Tumor-Associated Macrophages in Multiple Myeloma: Key Role in Disease Biology and Potential Therapeutic Implications. Curr Oncol. 2023 Jun 25;30(7):6111–33.

88. Huang R, Kang T, Chen S. The role of tumor-associated macrophages in tumor immune evasion. J Cancer Res Clin Oncol. 2024 May 7;150(5):238.

89. Zheng Y, Cai Z, Wang S, Zhang X, Qian J, Hong S, et al. Macrophages are an abundant component of myeloma microenvironment and protect myeloma cells from chemotherapy drug–induced apoptosis. Blood. 2009 Oct 22;114(17):3625–8.

90. Suyanı E, Sucak GT, Akyürek N, Şahin S, Baysal NA, Yağcı M, et al. Tumor-associated macrophages as a prognostic parameter in multiple myeloma. Ann Hematol. 2013 May;92(5):669–77.

91. Wang H, Hu W ming, Xia Z jun, Liang Y, Lu Y, Lin S xia, et al. High numbers of CD163+ tumor-associated macrophages correlate with poor prognosis in multiple myeloma patients receiving bortezomib-based regimens. J Cancer. 2019;10(14):3239–45.

92. Chen X, Chen J, Zhang W, Sun R, Liu T, Zheng Y, et al. Prognostic value of diametrically polarized tumor-associated macrophages in multiple myeloma. Oncotarget. 2017 Dec 22;8(68):112685–96.

93. Andersen MN, Andersen NF, Rødgaard-Hansen S, Hokland M, Abildgaard N, Møller HJ. The novel biomarker of alternative macrophage activation, soluble mannose receptor (sMR/sCD206): Implications in multiple myeloma. Leuk Res. 2015 Sep;39(9):971–5.

94. Andersen MN, Abildgaard N, Maniecki MB, Møller HJ, Andersen NF. Monocyte/macrophage-derived soluble CD 163: a novel biomarker in multiple myeloma. Eur J Haematol. 2014 Jul;93(1):41–7.

95. Botta C, GullÃ A, Correale P, Tagliaferri P, Tassone P. Myeloid-Derived Suppressor Cells in Multiple Myeloma: Pre-Clinical Research and Translational Opportunities. Front Oncol [Internet]. 2014 Dec 8 [cited 2024 Oct 15];4. Available from: http://journal.frontiersin.org/article/10.3389/fonc.2014.00348/abstract

96. Giannotta C, Autino F, Massaia M. The immune suppressive tumor microenvironment in multiple myeloma: The contribution of myeloid-derived suppressor cells. Front Immunol. 2023 Jan 16;13:1102471.

97. Bae MH, Park CJ, Suh C. Increased Monocytic Myeloid-Derived Suppressor Cells in Whole Blood Predict Poor Prognosis in Patients with Plasma Cell Myeloma. J Clin Med. 2021 Oct 14;10(20):4717.

98. Malek E, De Lima M, Letterio JJ, Kim BG, Finke JH, Driscoll JJ, et al. Myeloid-derived suppressor cells: The green light for myeloma immune escape. Blood Rev. 2016 Sep;30(5):341–8.

99. Harmer D, Falank C, Reagan MR. Interleukin-6 Interweaves the Bone Marrow Microenvironment, Bone Loss, and Multiple Myeloma. Front Endocrinol. 2019 Jan 8;9:788.

100. Wang JC, Sun L. PD-1/PD-L1, MDSC Pathways, and Checkpoint Inhibitor Therapy in Ph(-) Myeloproliferative Neoplasm: A Review. Int J Mol Sci. 2022 May 23;23(10):5837.

101. Perez C, Botta C, Zabaleta A, Puig N, Cedena MT, Goicoechea I, et al. Immunogenomic identification and characterization of granulocytic myeloid-derived suppressor cells in multiple myeloma. Blood. 2020 Jul 9;136(2):199–209.

102. Romano A, Parrinello NL, Simeon V, Puglisi F, La Cava P, Bellofiore C, et al. High-density neutrophils in MGUS and multiple myeloma are dysfunctional and immune-suppressive due to increased STAT3 downstream signaling. Sci Rep. 2020 Feb 6;10(1):1983.

103. Romano A, Laura Parrinello N, Cerchione C, Letizia Consoli M, Parisi M, Calafiore V, et al. The NLR and LMR ratio in newly diagnosed MM patients treated upfront with novel agents. Blood Cancer J. 2017 Dec 15;7(12):649.

104. Mu S, Ai L, Fan F, Sun C, Hu Y. Prognostic role of neutrophil–lymphocyte ratio in multiple myeloma: a dose–response meta-analysis. OncoTargets Ther. 2018 Jan;Volume 11:499–507.

105. Solmaz Medeni S, Acar C, Olgun A, Acar A, Seyhanlı A, Taskıran E, et al. Can Neutrophil-to-Lymphocyte Ratio, Monocyte-to-Lymphocyte Ratio, and Platelet-to-Lymphocyte Ratio at Day +100 be used as a prognostic marker in Multiple Myeloma patients with autologous transplantation? Clin Transplant. 2018 Sep;32(9):e13359.

106. Lee GW, Park SW, Go SI, Kim HG, Kim MK, Min CK, et al. The Derived Neutrophil-to-Lymphocyte Ratio Is an Independent Prognostic Factor in Transplantation Ineligible Patients with Multiple Myeloma. Acta Haematol. 2018;140(3):146–56.

107. Ratta M, Fagnoni F, Curti A, Vescovini R, Sansoni P, Oliviero B, et al. Dendritic cells are functionally defective in multiple myeloma: the role of interleukin-6. Blood. 2002 Jul 1;100(1):230–7.

108. Brimnes MK, Svane IM, Johnsen HE. Impaired functionality and phenotypic profile of dendritic cells from patients with multiple myeloma. Clin Exp Immunol. 2006 Feb 16;144(1):76–84.

109. Do TH, Johnsen HE, Kjærsgaard E, Taaning E, Svane IM. Impaired circulating myeloid DCs from myeloma patients. Cytotherapy. 2004 Jun;6(3):196–203.

110. Leone P, Berardi S, Frassanito MA, Ria R, De Re V, Cicco S, et al. Dendritic cells accumulate in the bone marrow of myeloma patients where they protect tumor plasma cells from CD8+ T-cell killing. Blood. 2015 Sep 17;126(12):1443–51.

111. Knight A, Rihova L, Kralova R, Penka M, Adam Z, Pour L, et al. Plasmacytoid Dendritic Cells in Patients with MGUS and Multiple Myeloma. J Clin Med. 2021 Aug 20;10(16):3717.

112. Ray A, Das DS, Song Y, Macri V, Richardson P, Brooks CL, et al. A novel agent SL-401 induces anti-myeloma activity by targeting plasmacytoid dendritic cells, osteoclastogenesis and cancer stem-like cells. Leukemia. 2017 Dec;31(12):2652–60.

113. Brown RD, Pope B, Murray A, Esdale W, Sze DM, Gibson J, et al. Dendritic cells from patients with myeloma are numerically normal but functionally defective as they fail to up-regulate CD80 (B7-1) expression after huCD40LT stimulation because of inhibition by transforming growth factor-β1 and interleukin-10. Blood. 2001 Nov 15;98(10):2992–8.

114. Cui C, Schoenfelt KQ, Becker KM, Becker L. Isolation of polymorphonuclear neutrophils and monocytes from a single sample of human peripheral blood. STAR Protoc. 2021 Dec;2(4):100845.

115. Botta C, Maia C, Garcés JJ, Termini R, Perez C, Manrique I, et al. FlowCT for the analysis of large immunophenotypic data sets and biomarker discovery in cancer immunology. Blood Adv. 2022 Jan 25;6(2):690–703.

116. Ragusa M, Santagati M, Mirabella F, Lauretta G, Cirnigliaro M, Brex D, et al. Potential Associations Among Alteration of Salivary miRNAs, Saliva Microbiome Structure, and Cognitive Impairments in Autistic Children. Int J Mol Sci. 2020 Aug 27;21(17):6203.

117. Bolyen E, Rideout JR, Dillon MR, Bokulich NA, Abnet CC, Al-Ghalith GA, et al. Reproducible, interactive, scalable and extensible microbiome data science using QIIME 2. Nat Biotechnol. 2019 Aug;37(8):852–7.

118. Bokulich NA, Subramanian S, Faith JJ, Gevers D, Gordon JI, Knight R, et al. Quality-filtering vastly improves diversity estimates from Illumina amplicon sequencing. Nat Methods. 2013 Jan;10(1):57–9.

119. Ernst F, Shetty S, Borman T, Lahti L. mia: Microbiome analysis. 2024;

120. Borman T, Ernst F, Lahti L. miaViz: Microbiome Analysis Plotting and Visualization. 2024;

121. Peschel S, Müller CL, Von Mutius E, Boulesteix AL, Depner M. NetCoMi: network construction and comparison for microbiome data in R. Brief Bioinform. 2021 Jul 20;22(4):bbaa290.

122. Xu S, Zhan L, Tang W, Wang Q, Dai Z, Zhou L, et al. MicrobiotaProcess: A comprehensive R package for deep mining microbiome. The Innovation. 2023 Mar;4(2):100388.

123. Shannon P, Markiel A, Ozier O, Baliga NS, Wang JT, Ramage D, et al. Cytoscape: A Software Environment for Integrated Models of Biomolecular Interaction Networks. Genome Res. 2003 Nov;13(11):2498–504.

124. Tirosh I, Izar B, Prakadan SM, Wadsworth MH, Treacy D, Trombetta JJ, et al. Dissecting the multicellular ecosystem of metastatic melanoma by single-cell RNA-seq. Science. 2016 Apr 8;352(6282):189–96.

125. Boiarsky R, Haradhvala NJ, Alberge JB, Sklavenitis-Pistofidis R, Mouhieddine TH, Zavidij O, et al. Single cell characterization of myeloma and its precursor conditions reveals transcriptional signatures of early tumorigenesis. Nat Commun. 2022 Nov 17;13(1):7040.

126. VanderWall K, Daniels-Wells TR, Penichet M, Llichtenstein A. Iron in Multiple Myeloma. Crit Rev Oncog. 2013;18(5):449–61.

127. Song MK, Chung JS, Seol YM, Shin HJ, Choi YJ, Cho GJ. Elevation of Serum Ferritin is Associated with the Outcome of Patients with Newly Diagnosed Multiple Myeloma. Korean J Intern Med. 2009;24(4):368.

128. Zhang Y, Pan J, Chen X, Wang L, Chen L, Tian Y, et al. Dynamic Monitoring of Serum Ferritin As An Adverse Prognostic Biomarker in Patients with Multiple Myeloma. Biomark Med. 2021 Nov;15(16):1541–51.

129. Strasser-Weippl K, Ludwig H. Ferritin as prognostic marker in multiple myeloma patients undergoing autologous transplantation. Leuk Lymphoma. 2014 Nov 2;55(11):2520–4.

130. Campanella A, Santambrogio P, Fontana F, Frenquelli M, Cenci S, Marcatti M, et al. Iron increases the susceptibility of multiple myeloma cells to bortezomib. Haematologica. 2013 Jun 1;98(6):971–9.

131. Deseke M, Prinz I. Ligand recognition by the γδ TCR and discrimination between homeostasis and stress conditions. Cell Mol Immunol. 2020 Sep;17(9):914–24.

132. Willcox BE, Willcox CR. γδ TCR ligands: the quest to solve a 500-million-year-old mystery. Nat Immunol. 2019 Feb;20(2):121–8.

133. Hu Y, Hu Q, Li Y, Lu L, Xiang Z, Yin Z, et al. γδ T cells: origin and fate, subsets, diseases and immunotherapy. Signal Transduct Target Ther. 2023 Nov 22;8(1):434.

134. Corsale AM, Di Simone M, Dieli F, Meraviglia S. Where could gammadelta T cells take us in the treatment of cancer? Expert Opin Biol Ther. 2023 Jan 2;23(1):1–5.

135. Lo Presti E, Corsale AM, Dieli F, Meraviglia S. γδ cell-based immunotherapy for cancer. Expert Opin Biol Ther. 2019 Sep 2;19(9):887–95.

136. Arias-Badia M, Chang R, Fong L. γδ T cells as critical anti-tumor immune effectors. Nat Cancer. 2024 Jul 26;5(8):1145–57.

137. Wang CQ, Lim PY, Tan AHM. Gamma/delta T cells as cellular vehicles for anti-tumor immunity. Front Immunol. 2024 Jan 11;14:1282758.

138. Fiala GJ, Lücke J, Huber S. Pro- and antitumorigenic functions of γδ T cells. Eur J Immunol. 2024 Aug;54(8):2451070.

139. Gentles AJ, Newman AM, Liu CL, Bratman SV, Feng W, Kim D, et al. The prognostic landscape of genes and infiltrating immune cells across human cancers. Nat Med. 2015 Aug;21(8):938–45.

140. Yi M, Li T, Niu M, Zhang H, Wu Y, Wu K, et al. Targeting cytokine and chemokine signaling pathways for cancer therapy. Signal Transduct Target Ther. 2024 Jul 22;9(1):176.

141. Zhang L, Xiang Y, Li Y, Zhang J. Gut microbiome in multiple myeloma: Mechanisms of progression and clinical applications. Front Immunol. 2022 Dec 8;13:1058272.

142. Jian X, Zhu Y, Ouyang J, Wang Y, Lei Q, Xia J, et al. Alterations of gut microbiome accelerate multiple myeloma progression by increasing the relative abundances of nitrogen-recycling bacteria. Microbiome. 2020 Dec;8(1):74.

143. Ahmed N, Ghannoum M, Gallogly M, De Lima M, Malek E. Influence of gut microbiome on multiple myeloma: friend or foe? J Immunother Cancer. 2020 Jun;8(1):e000576.

144. Liang X, Guo X, Jin H, Shen L, Ding L, Guan X, et al. Changes in the intestinal microbiota of multiple myeloma patients living in high-altitude and cold regions analyzed using 16s rRNA high-throughput sequencing. Exp Ther Med. 2024 Apr 29;27(6):269.

145. Brevi A, Cogrossi LL, Lorenzoni M, Mattorre B, Bellone M. The Insider: Impact of the Gut Microbiota on Cancer Immunity and Response to Therapies in Multiple Myeloma. Front Immunol. 2022 Mar 17;13:845422.

146. Kumar S, Paiva B, Anderson KC, Durie B, Landgren O, Moreau P, et al. International Myeloma Working Group consensus criteria for response and minimal residual disease assessment in multiple myeloma. Lancet Oncol. 2016 Aug;17(8):e328–46.

147. Paiva B, García-Sanz R, San Miguel JF. Multiple Myeloma Minimal Residual Disease. In: Roccaro AM, Ghobrial IM, editors. Plasma Cell Dyscrasias [Internet]. Cham: Springer International Publishing; 2016 [cited 2024 Oct 9]. p. 103–22. (Cancer Treatment and Research; vol. 169). Available from: http://link.springer.com/10.1007/978-3-319-40320-5_7

148. Szalat R, Anderson K, Munshi N. Role of minimal residual disease assessment in multiple myeloma. Haematologica [Internet]. 2024 Feb 8 [cited 2024 Oct 9]; Available from: https://haematologica.org/article/view/haematol.2023.284662

149. Cavo M, San-Miguel J, Usmani SZ, Weisel K, Dimopoulos MA, Avet-Loiseau H, et al. Prognostic value of minimal residual disease negativity in myeloma: combined analysis of POLLUX, CASTOR, ALCYONE, and MAIA. Blood. 2022 Feb 10;139(6):835–44.

150. Guerrero C, Puig N, Cedena MT, Goicoechea I, Perez C, Garcés JJ, et al. A Machine Learning Model Based on Tumor and Immune Biomarkers to Predict Undetectable MRD and Survival Outcomes in Multiple Myeloma. Clin Cancer Res. 2022 Jun 13;28(12):2598–609.

Candidate's contributions

Publications

Additionally, during my PhD, the following scientific articles were published in international journals:

Corsale AM*, Di Simone M*, Dieli F, Meraviglia S. γδ T cell immunotherpy: Requirment of combination? γδ T Cell Cancer Immunotherapy: Evidence-Based Perspectives for Clinical Translation (Breaking Tolerance to Anti-Cancer Cell-Mediated Immunotherapy), vol. 7, 61-76, Elsevier Science Publishing Co Inc 2024. doi: 10.1016/B978-0-443-21766-1.00010-2 (*These authors contributed equally).

Corsale AM, Di Simone M, Meraviglia S, Caruso C. γδ T-Cell Immunophenotype for the Study of Human Aging. Immunosenescence: Methods and Protocols, Methods in Molecular Biology, vol. 2857, doi: 10.1007/978-1-0716-4128-6_5

Gigliotta E, Plano F, Corsale G, **Corsale AM**, Aquilina C, Speciale M, Rizzuto A, Martino EA, Leotta D, Solimando AG, Ria R, Gentile M, Siragusa S, Botta C. Measurable therapeutic antibody in serum as potential predictive factor of response to anti-CD38 therapy in non-IgG-k myeloma patients. Exp Hematol Oncol. 2024 Aug 6;13(1):82. doi: 10.1186/s40164-024-00547-x.

Di Simone M*, **Corsale AM***, Toia F*, Shekarkar Azgomi M, Di Stefano AB, Lo Presti E, Cordova A, Montesano L, Dieli F, Meraviglia S. Tumor-infiltrating γδ T cells as targets of immune checkpoint blockade in melanoma. J Leukoc Biol. 2024 Mar 29;115(4):760-770. doi: 10.1093/jleuko/qiae023. (*These authors contributed equally).

Plano F, Shekarkar Azgomi M, **Corsale AM**, Spoto C, Caccamo N, Meraviglia S, Dieli F, D'Angelo P, Trizzino A, Siragusa S. Humoral and Cell-Mediated Responses to SARS-CoV-2 Vaccination in a Cohort of Immunodeficient Patients. Hematol Rep. 2023 Dec 8;15(4):707-716. doi: 10.3390/hematolrep15040071.

Ligotti ME, Accardi G, Aiello A, Calabrò A, Caruso C, **Corsale AM**, Dieli F, Di Simone M, Meraviglia S, Candore G. Sicilian Semi- and Supercentenarians: Age-related NK Cell Immunophenotype and Longevity Trait Definition. Transl Med UniSa. 2023 Oct 17;25(1):11-15. doi: 10.37825/2239-9747.1041.

Ligotti ME, Accardi G, Aiello A, Calabrò A, Caruso C, **Corsale AM**, Dieli F, Di Simone M, Meraviglia S, Candor G. Sicilian semi- and supercentenarians: age-related T γδ cell immunophenotype contributes to longevity trait definition. Clin Exp Immunol. 2023 Dec 8:uxad132. doi: 10.1093/cei/uxad132.

Ligotti ME, Accardi G, Aiello A, Aprile S, Calabrò A, Caldarella R, Caruso C, Ciaccio M, **Corsale AM**, Dieli F, Di Simone M, Giammanco GM, Mascarella C, Akbar AN, Meraviglia S, Candore G. Sicilian semi- and supercentenarians: identification of age-related T cell immunophenotype to define longevity trait. Clin Exp Immunol. 2023 Jul 3:uxad074. doi: 10.1093/cei/uxad074.

Urzì, O, Cafora M, Rabienezhad Ganji N, Tinnirello V, Gasparro R, Raccosta S, Manno M, **Corsale AM**, Conigliaro A, Pistocchi A, Raimondo S, Alessandro R (2023), Lemon-derived nanovesicles achieve antioxidant and anti-inflammatory effects activating the AhR/Nrf2 signaling pathway, iScience, Volume 26, Issue 7, 107041. doi: 10.1016/j.isci.2023.107041

Toia F, Lo Presti E, Di Stefano AB, Di Simone M, Trapani M, **Corsale AM**, Picone C, Moschella F, Dieli F, Cordova A, Meraviglia S (2023). An analysis of the immunomodulatory properties of human spheroids from adipose-derived stem cells. Life Sci, 321:121610. doi: 10.1016/j.lfs.2023.121610.

Corsale AM*, Di Simone M*, Lo Presti E, Dieli F, Meraviglia S (2023) γδ T cells and their clinical application in colon cancer. Front. Immunol. 14:1098847. doi: 10.3389/fimmu.2023.1098847 (*These authors contributed equally)

Corsale AM*, Di Simone M*, Dieli F, Meraviglia S (2023), Where could gammadelta T cells take us in the treatment of cancer? Expert Opinion on Biological Therapy, 23:1, 1-5, doi: 10.1080/14712598.2022.2147424 (*These authors contributed equally)

Di Simone M*, **Corsale AM***, Lo Presti E, Scichilone N, Picone C, Giannitrapani L, Dieli F, Meraviglia S (2022), Phenotypical and Functional Alteration of γδ T Lymphocytes in COVID-19 Patients: Reversal by Statins. Cells,11(21):3449. doi: 10.3390/cells11213449 (*Questi autori hanno contribuito equamente)

Ippolito M, Spurio G, Compagno V, Rizzo A, Di Simone M, **Corsale AM**, Mazzola G, Giarratano A, Meraviglia S, Cortegiani A, Alongi A (2022), Autologous conditioned serum for chronic pain in patients with osteoarthritis: A feasibility observational study. British Journal of Pain. doi:10.1177/20494637221134169

Raimondo S, Urzì O, Meraviglia S, Di Simone M, **Corsale AM**, Rabienezhad Ganji N, Palumbo Piccionello A, Polito G, Lo Presti E, Dieli F, Conigliaro A, Alessandro R (2022), Anti-inflammatory properties of lemon-derived extracellular vesicles are achieved through the inhibition of ERK/NF-κB signalling pathways. J Cell Mol Med., 26: 4195-4209. doi: 10.1111/jcmm.17404

Awards

- NIBIT Science Award at the XXI NIBIT Meeting (Palermo (Italy), October 17-19, 2024)
- Travel grant to attend the 5th European Myeloma Network Meeting (EMN) (Turin (Italy), April 18-20, 2024).
- Abstract Achievement Award at 64th ASH Annual Meeting and Exposition (New Orleans (Louisiana), December 10-13, 2022).

Conference talks

The results achieved during my PhD have been presented as oral presentations at numerous conferences.

Dysfunctional bone marrow and circulating γδ T cells were indicators of a higher probability of advancing from pre-malignant plasma cell dyscrasias to symptomatic multiple myeloma

21st NIBIT Meeting, Palermo (Italy), October 17-19, 2024

Dysfunctional bone marrow and circulating γδ T cells were indicative of an increased likelihood of transitioning from pre-malignant plasma cell dyscrasias to symptomatic multiple myeloma

XVIII National Congress of the Italian Society of Experimental Hematology (SIES), Florence (Italy), March 7-9, 2024

T cell modulation along myeloma evolution

Myeloma2023, Palermo (Italy), September 21-22, 2023

The immunological composition of bone marrow reflects the progression of multiple myeloma and determines patient outcome.

CD38 in Basic Science and Clinical Practice, Bergamo (Italy), July 3-15, 2023

Bone marrow infiltrating γδ T Cells acquired an exhausted phenotype during multiple myeloma evolution

2nd School of Multiple Myeloma, Rome (Italy), June 30 – July 1, 2022

Poster presentation

The results achieved during my PhD have been presented as poster presentations at numerous national and international conferences.

Corsale AM, Shekarkar Azgomi M, M. Di Simone M, Gigliotta E, Rizzuto A, Speciale M, Aquilina C, Biondo M, Romano A, Romano A, Neri A, Caccamo N, Dieli F, Meraviglia S, Siragusa S, Botta C. Immune system dysfunction and gut microbiota composition across multiple myeloma progression from premalignant conditions. 21st NIBIT Meeting, Palermo (Italy), October 17-19, 2024

Rizzuto A, Speciale M, **Corsale AM**, Aquilina C, Gigliotta E, Merenda A, Vasta S, Tomaselli CA, Sciortino M, Brucato F, Caccamo N, Dieli F, Siragusa S, Meraviglia S, Botta C. Flow cytometry-based minimal residual disease assessment and immune correlates in multiple myeloma: a real-world experience. 51st National Congress of the Italian Society of Hematology (SIE), Milan (Italy), September 23-25, 2024.

Corsale AM, Shekarkar Azgomi M, M. Di Simone M, Gigliotta E, Speciale M, Sciortino M, Aquilina C, Biondo M, Romano A, Neri A, Santagati M, Caccamo N, Dieli F, Meraviglia S, Siragusa S, Botta C. Mapping immune system dysfunction and gut microbiota composition throughout the evolution of multiple myeloma from premalignant conditions. 51st National Congress of the Italian Society of Hematology (SIE), Milan (Italy), September 23-25, 2024.

Corsale AM, Shekarkar Azgomi M, M. Di Simone M, Gigliotta E, Speciale M, Sciortino M, Aquilina C, Biondo M, Romano A, Neri A, Santagati M, Vertillo Aluisio G, Privitera GF, Caccamo N, Dieli F, Meraviglia S, Siragusa S, Botta C. Deciphering the interplay of immune alterations and microbiome

changes along multiple myeloma evolution from premalignant conditions. 21st International Myeloma Society Annual Meeting (IMS), Rio de Janeiro (Brazil), September 25-28, 2024.

Corsale AM, M. Di Simone M, Shekarkar Azgomi M, Gigliotta E, Rizzuto A, Garofano F, Speciale M, Sciortino M, Aquilina C, Brucato F, Dieli C, Corsale G, Buffa F, Caccamo N, Siragusa S, Dieli F, Meraviglia S, Botta C. Bone marrow immune profiles and their predictive value in multiple myeloma progression and treatment response. 7th European Congress of Immunology (ECI), Dublin (Irland), September 1-4, 2024.

Corsale AM, Shekarkar Azgomi M, Gigliotta E, Rizzuto A, M. Di Simone M, Garofano F, Speciale M, Sciortino M, Aquilina C, Brucato F, Corsale G, Buffa F, Caccamo N, Dieli F, Meraviglia S, Siragusa S, Botta C. Bone marrow myeloid precursors predict tumor evolution and response to anti-CD38 antibodies in multiple myeloma patients. 29th European Hematology Association (EHA), Madrid (Spain), June 13-16, 2024.

Corsale AM, M. Di Simone M, Shekarkar Azgomi M, Gigliotta E, Rizzuto A, Garofano F, Speciale M, Sciortino M, Aquilina C, Brucato F, Corsale G, Buffa F, Caccamo N, Siragusa S, Dieli F, Meraviglia S, Botta C. Immune cell landscape within the bone marrow: a roadmap from MGUS to active multiple myeloma and treatment responsiveness. 6th International Conference Translational Immunology, Monopoli (Bari), May 22-25, 2024.

Corsale AM, Shekarkar Azgomi M, Gigliotta E, Di Simone M, Rizzuto A, Garofano F, Speciale M, Sciortino M, Aquilina C, Romano A, Brucato F, Corsale G, Cambria D, Neri F, Buffa F, Caccamo N, Dieli F, Meraviglia S, Siragusa S, Botta C. Immune cell landscape within the bone marrow: a roadmap from MGUS to active multiple myeloma and treatment responsiveness. 5th European Myeloma Network Meeting (EMN), Turin (Italy), April 18-20, 2024.

Corsale AM, Di Simone M, Shekarkar Azgomi M, Speciale M, Gigliotta E, Garofano F, Aquilina C, Vullo C, Santagati M, Caccamo N, Romano A, Dieli F, Meraviglia S, Siragusa S, Botta C. Immune system, cytokine profiles, and fecal microbiota changes influence the progression from monoclonal gammopathy of undetermined significance (MGUS) to multiple myeloma (MM). XVIII Congress of the Italian Society of Experimental Hematology (SIES), Florence (Italy), March 7-9, 2024. Haematologica 2024;109(s1):1-134.

Corsale AM, Di Simone M, Shekarkar Azgomi M, Speciale M, Gigliotta E, Garofano F, Aquilina C, Vullo C, Caccamo N, Dieli F, Meraviglia S, Siragusa S, Botta C. Immune Cells, Cytokines, and Gut Microbiota Landscape along Monoclonal Gammopathy of Undetermined Significance (MGUS) to Multiple Myeloma (MM) Evolution. 65th ASH Annual Meeting and Exposition, San Diego (California), December 9-12, 2023.
Blood 2023; 142 (Supplement 1): 3292.doi: https://doi.org/10.1182/blood-2023-189847

Corsale AM, Shekarkar Azgomi M, Plano F, Di Simone M, Perez C, Picone C, Gigliotta E, Speciale M, Vullo C, Camarda G, Rotolo C, Santoro M, Caccamo N, Paiva B, Siragusa S, Dieli F, Meraviglia S, Botta C. The composition of immune cells in bone marrow reflects the progression of multiple myeloma and influences treatment response. 50th National Congress of the Italian Society of Hematology (SIE), Rome (Italy), October 23-25, 2023.

Corsale AM, Shekarkar Azgomi M, Plano F, Di Simone M, Perez C, Picone C, Gigliotta E, Speciale M, Vullo C, Camarda G, Rotolo C, Santoro M, Caccamo N, Paiva B, Siragusa S, Dieli F, Meraviglia S, Botta C. A high risk of progression from smoldering to symptomatic multiple myeloma was predicted by bone marrow and circulating $\gamma\delta$ T cells. 20th International Myeloma Society Annual Meeting, Athens (Greece) September 27-30, 2023.

Corsale AM, Shekarkar Azgomi M, Gigliotta E, Plano F, Di Simone M, Speciale M, Vullo C, Sciortino M, Brucato F, Buffa F, Caccamo N, Dieli F, Meraviglia S, Siragusa S, Botta C. Bone marrow immune composition reflects multiple myeloma evolution and influences patients' outcome. 20th International Myeloma Society Annual Meeting, Athens (Greece) September 27-30, 2023.

Corsale AM, Shekarkar Azgomi M, Plano F, Di Simone M, Perez C, Picone C, Gigliotta E, Speciale M, Vullo C, Camarda G, Rotolo C, Santoro M, Caccamo N, Paiva B, Siragusa S, Dieli F, Meraviglia S, Botta C. Bone marrow and circulating γδ T cells predict high risk of progression from smoldering to symptomatic multiple myeloma. 10th international γδ T cell conference, Lisbon (Portugal), June 20-23 June, 2023.

Corsale AM, Shekarkar Azgomi M, Plano F, Di Simone M, Perez C, Picone C, Gigliotta E, Speciale M, Vullo C, Camarda G, Rotolo C, Santoro M, Caccamo N, Paiva B, Siragusa S, Dieli F, Meraviglia S, Botta C. Bone marrow and circulating γδ T cells predict high risk of progression from smoldering to symptomatic multiple myeloma. XIV National Congress of SIICA, Verona (Italy), May 22-25, 2023.

Corsale AM, Shekarkar Azgomi M, Plano F, Di Simone M, Perez C, Picone C, Gigliotta E, Vullo C, Camarda G, Rotolo C, Speciale M, Santoro M, Caccamo N, Dieli F, Paiva B, Meraviglia S, Siragusa S, Botta C. High TIM-3 Expression May Contribute to the Functional Impairment of Bone Marrow and Circulating Gamma Delta T Lymphocytes during the Progression of Multiple Myeloma. 64th ASH Annual Meeting and Exposition, New Orleans (Louisiana), December 10-13, 2022.
Blood 2022; 140 (Supplement 1): 9943–9944. doi:10.1182/blood-2022-167131

Corsale AM, Shekarkar Azgomi M, Plano F, Di Simone M, Perez C, Picone C, Gigliotta E, Vullo C, Camarda G, Rotolo C, Santoro M, Caccamo N, Dieli F, San Miguel J, Paiva B, Meraviglia S, Siragusa S, Botta C. Single-cell analysis of bone marrow γδ lymphocytes during the evolution of multiple myeloma demonstrates the early acquisition of an exhausted phenotype. 49th National Congress of the Italian Society of Hematology (SIE), Rome (Italy), September 26-28, 2022.

Acknowledgments

First and foremost, I would like to express my profound gratitude to my supervisors, Professors Cirino Botta and Serena Meraviglia. Their expert guidance, steadfast encouragement, and invaluable insights have been instrumental throughout my doctoral research journey. Their unwavering support and thoughtful feedback challenged me to exceed my expectations and achieve more than I ever thought possible.

I am also deeply thankful to my colleagues and friends at CLADIBIOR. The shared experiences, collaborative spirit and mutual support within this group have been vital to my personal and professional growth. I feel incredibly fortunate to have had such a dedicated and inspiring network around me.

Lastly, I am immensely grateful to my family. Your unwavering love, patience, and encouragement have been my foundation, giving me the strength to persevere through every challenge. This achievement is as much yours as it is mine.